nature nanotechnology

SUPPLEMENTARY INFORMATION

https://doi.org/10.1038/s41565-018-0109-z

In the format provided by the authors and unedited.

A bio-hybrid DNA rotor–stator nanoengine that moves along predefined tracks

Julián Valero[1,2], Nibedita Pal[3], Soma Dhakal[3,4], Nils G. Walter[3] and Michael Famulok[1,2]*

[1]LIMES Program Unit Chemical Biology & Medicinal Chemistry, c/o Kekulé Institut für Organische Chemie und Biochemie, University of Bonn, Bonn, Germany. [2]Center of Advanced European Studies and Research (CAESAR), Bonn, Germany. [3]Single Molecule Analysis Group, Department of Chemistry, University of Michigan, Ann Arbor, MI, USA. [4]Present address: Department of Chemistry, Virginia Commonwealth University, Richmond, VA, USA. *e-mail: m.famulok@uni-bonn.de

Supplementary Information

A bio-hybrid DNA rotor/stator nanoengine that moves along predefined tracks

Julián Valero, Nibedita Pal, Soma Dhakal, Nils G. Walter, & Michael Famulok

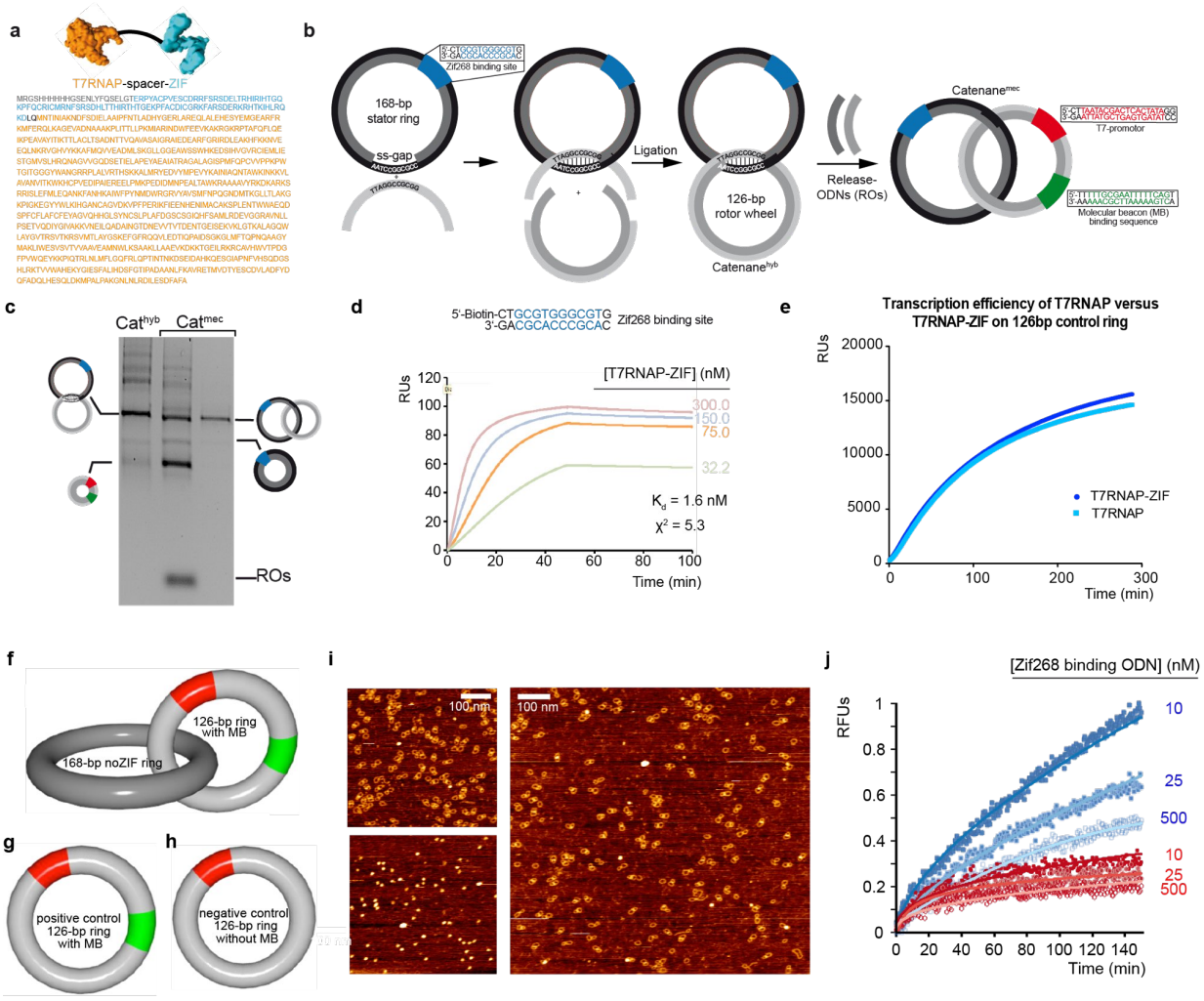

Supplementary Fig. 1. Assembly of the catenane nanoengine, transcription activity, binding affinity, and control experiments (**a**) Amino acid sequence of T7RNAP-ZIF. (**b**) Design, and schematic assembly of the non-symmetrical DNA catenane. (**c**) Analytical agarose gel of the assembled non-symmetric catenane. Lane 1, pseudocatenane, lane 2, catenane after addition of ROs. (**d**) Surface plasmon resonance binding studies of T7RNAP-ZIF in presence of the Zif268 targeting sequence. (**e**) Transcription activity of engineered T7RNAP-ZIF compared with commercial T7RNAP in presence of the circular 126-bp ring rotor template. (**f-h**) Schematic representation of the DNA catenane structure lacking (**f**) the Zif268 binding site and representation of 126-bp rotor rings containing (**g**, positive control) or lacking (**h**, negative control) the sequence encoding the molecular beacon binding site. (**i**) AFM images of the DNA catenane lacking the Zif268 binding domain (upper left), the T7RNAP-ZIF (lower left) and the combination of both (right). (**j**) Fluorescence kinetics of the RCT performed by the catenane (blue) and the control catenane (red) at different equivalents of zinc finger binding motif as indicated (10, 25, 500 nM), in the presence of T7RNAP-ZIF.

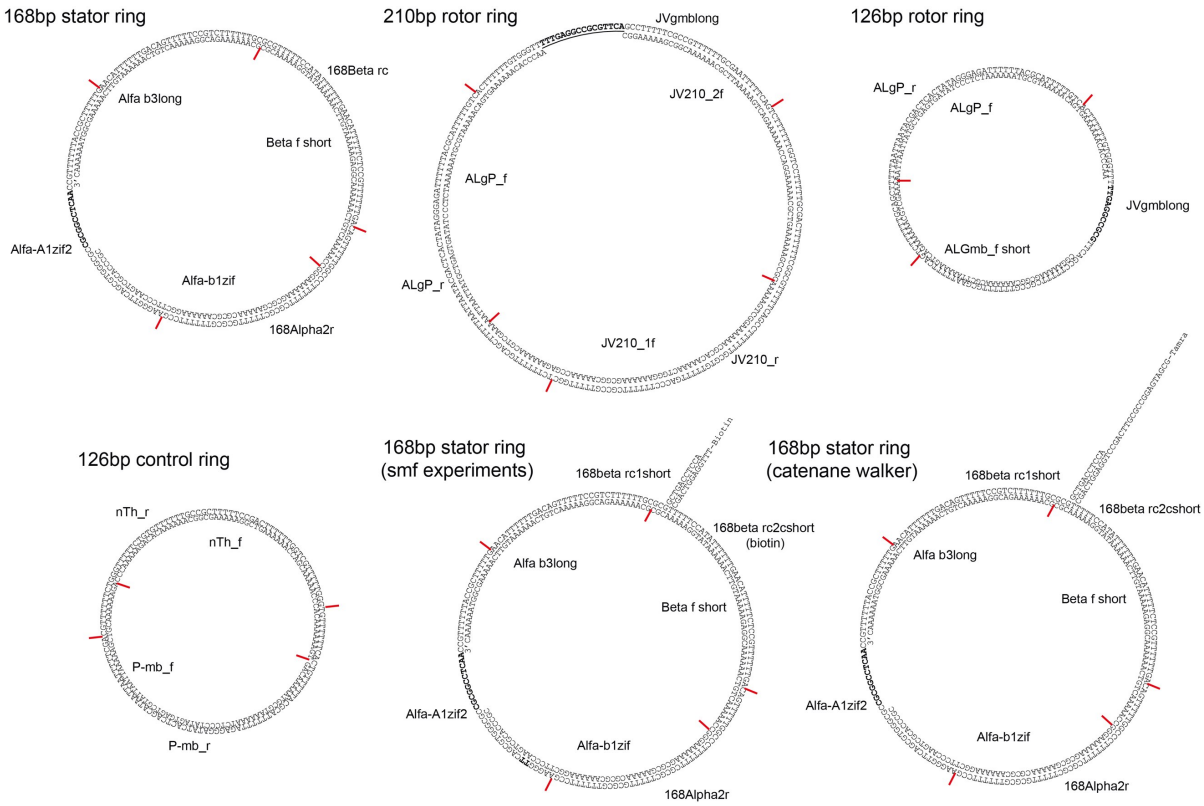

Supplementary Fig. 2. Secondary structure of all DNA rings used in this study, including the names of the ODNs used for the assembly.

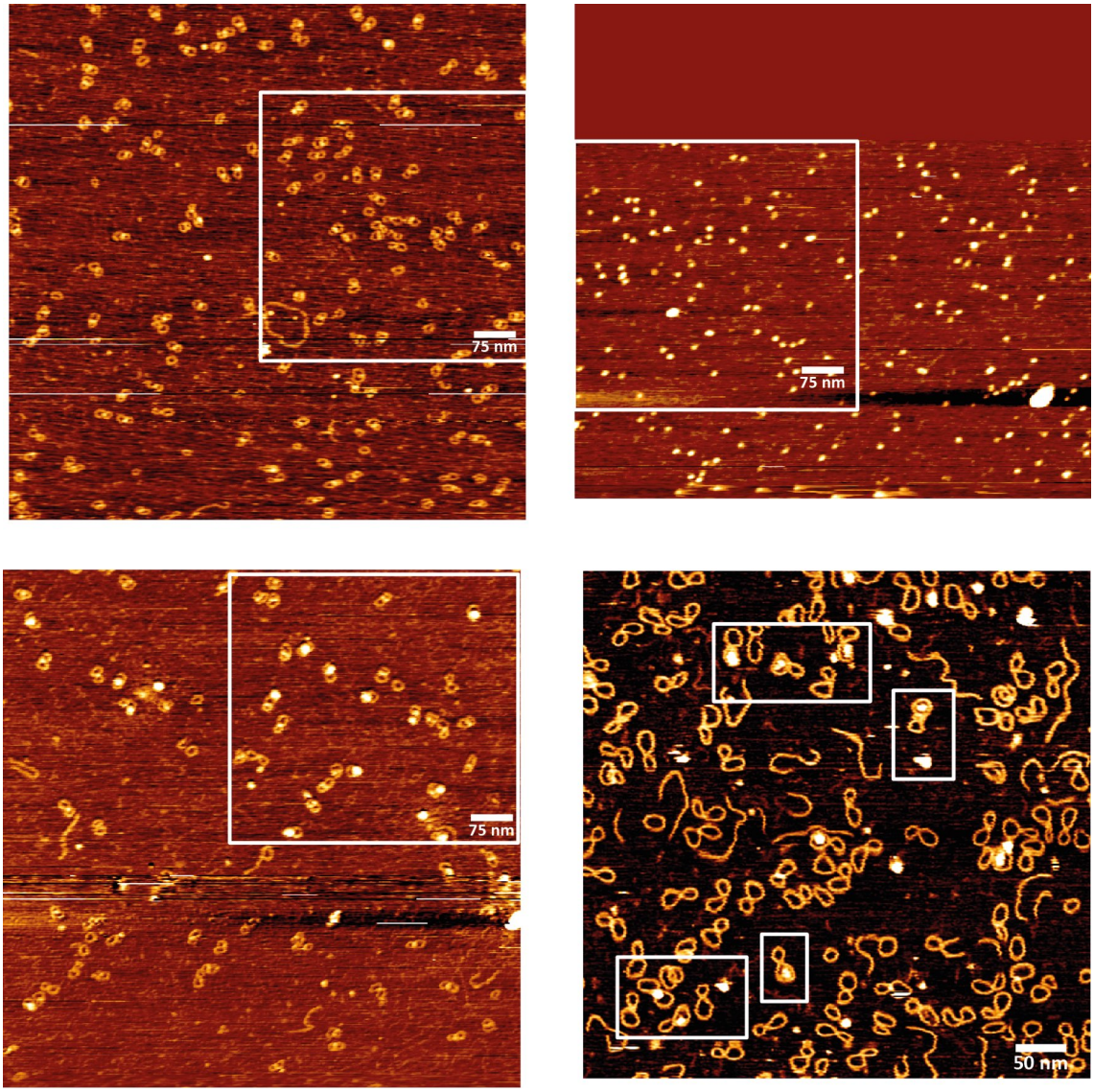

Supplementary Fig. 3. Larger sections from the uncropped AFM images used for the panels in Figure 1.

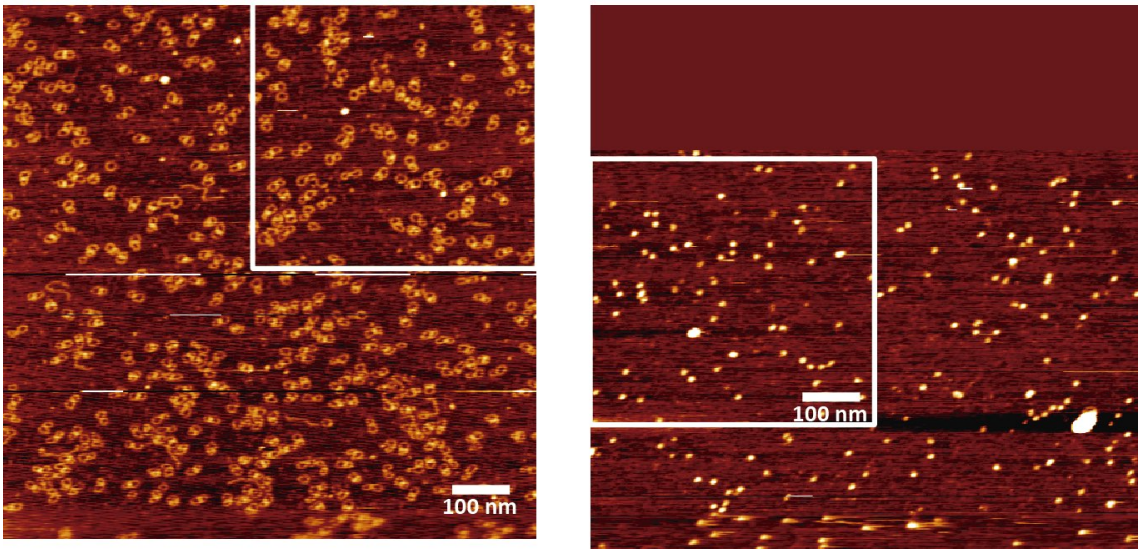

Supplementary Fig. 4. Larger sections from the uncropped AFM images used for the panels in Suppl. Fig. 1.

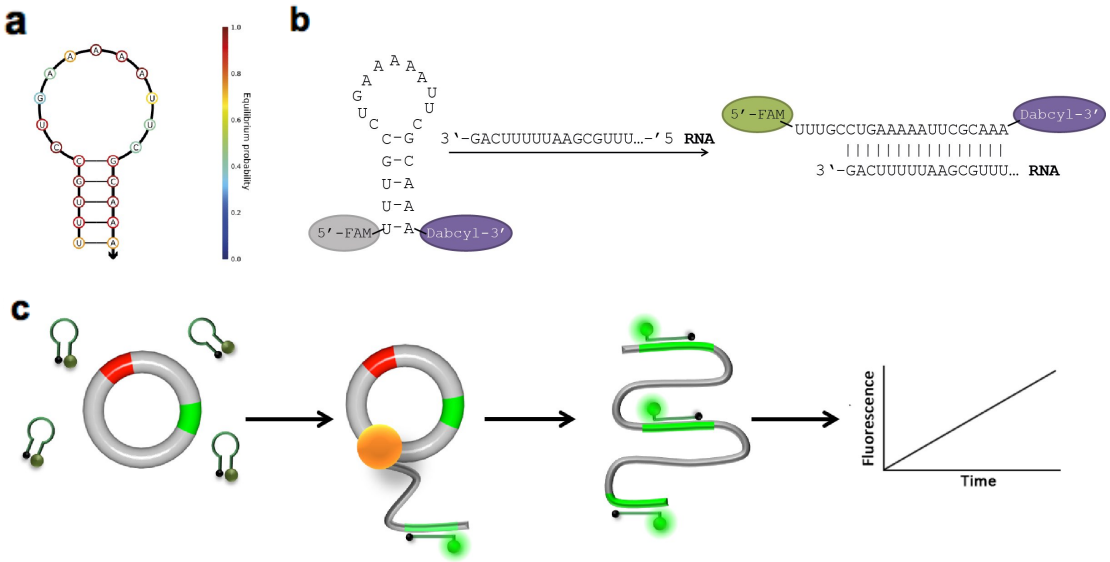

Supplementary Fig. 5. Folding, structure, and hybridization scheme of the molecular beacon (MB) used in this study. (**a**) Intramolecular folding patter of MB calculated by Nupack[1] (using Mathews et al., 1999 RNA energy parameters)[2] at 37 ºC. The probability of the given configuration at each site is color coded from 0 (blue) to 1 (red). (**b**) Molecular beacon hybridization. An RNA fragment produced during rolling circle transcription opens the hairpin structure of the MB (2'-O-Me-RNA), forms the duplex and thus, gives rise to an increase of FAM fluorescence signal. (**c**) Working principle of the molecular beacon fluorescence assay during rolling circle transcription of a DNA ring template.

a

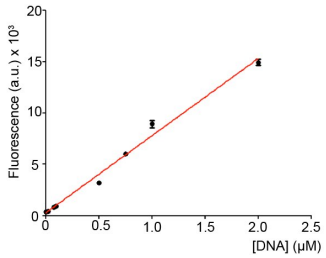

b

ZIF-Catenane	5 nM	10 nM	noZIF-Catenane	5 nM	10 nM	MB-Ring	5 nM	10 nM
Experiment 1	2106	3022	Experiment 1	1160	1703	Experiment 1	882	1637
Experiment 2	1362	2214	Experiment 2	613	922	Experiment 2	1143	1590
Experiment 3	2446	4241	Experiment 3	820	1443	Experiment 3	1150	1732
mean	1971	3159	mean	864	1356	mean	1058	1653
sd	554	1020	sd	276	398	sd	153	72
μmoles	0.23	0.38	μmoles	0.08	0.14	μmoles	0.10	0.18
total copies	45	38	total copies	16	14	total copies	21	18
rpm	**0.23**	**0.20**	**rpm**	**0.08**	**0.07**	**rpm**	**0.11**	**0.09**

Supplementary Fig. 6. Calibration and quantification of the RNA produced during rolling circle transcription and kinetic analysis by molecular beacon fluorescence experiments. (**a**) Calibration curve for the molecular beacon at increasing concentrations of the complementary ODN (JVgmblong_RO). (**b**) Analysis of the amount of RNA copies generated and the rpm values obtained for ZIF-catenane, the noZIF-catenane, and the MB-ring control (see Suppl. Fig. 7).

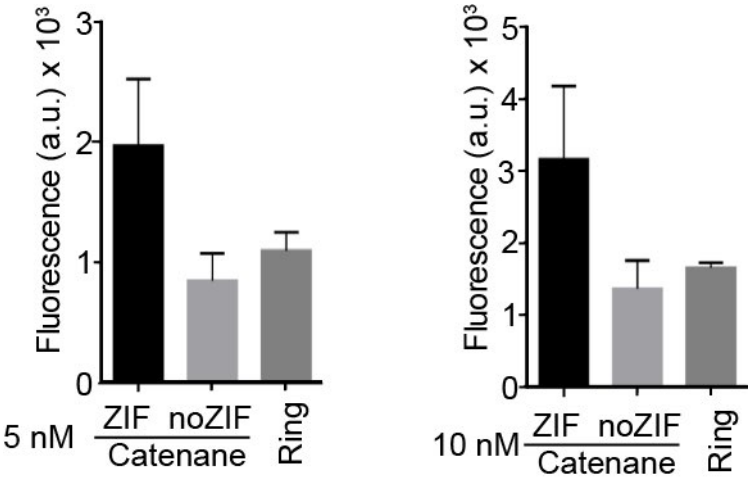

Supplementary Fig. 7. Kinetic analysis of the molecular beacon transcription assay. Fluorescence signal obtained after the molecular beacon transcription assay for the ZIF-catenane, the noZIF-catenane, and the MB-ring control at 5 and 10 nM template concentrations, respectively. Error bars: n = 9, mean ±SD

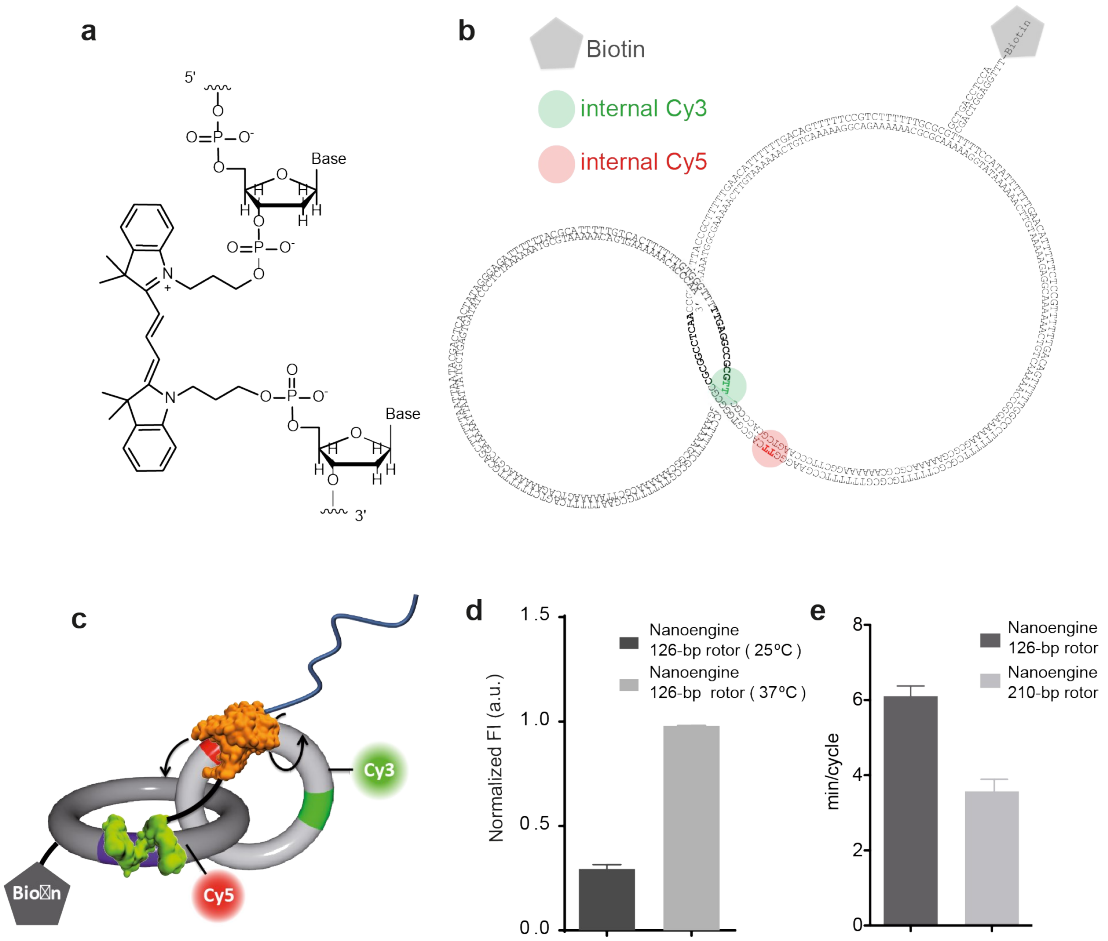

Supplementary Fig. 8. Fluorophore labelling strategy and microscope setup for the sm-FRET experiments (**a**) Chemical structure of the internal Cy3 fluorescent label used in this study, which is located in the DNA backbone between two phosphodiester groups. (**b**) Detailed representation of the DNA catenane used for smFRET experiments and the specific sequence location of the Cy3, Cy5 and biotin labels. (**c**) Scheme of the DNA catenane motor labelled with donor (Cy3, rotor) and acceptor (Cy5, stator) FRET pairs and a biotin molecule for immobilization on a streptavidin-coated glass surface to perform smFRET studies. (**d**) Molecular beacon fluorescence experiment carried out at 25ºC and 37ºC with the nanoengine having the 126-bp rotor ring. (**e**) Rotational speed assessed by bulk fluorescence experiments at 25ºC of the labelled nanoengines containing either 126-bp or 210-bp rotor rings. Error bars: n = 3, mean ±SD

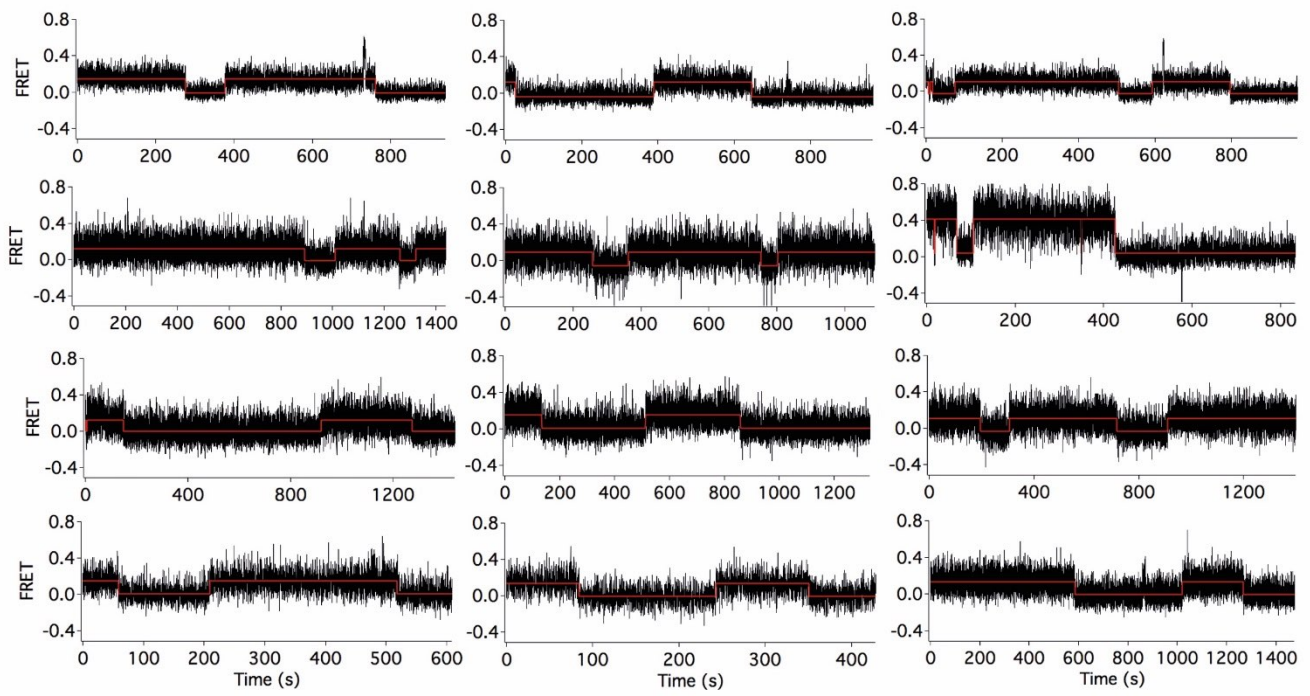

Supplementary Fig. 9. Representative smFRET trajectories with more than one-and-a-half full transcription cycles representing continuous T7RNAP-ZIF operation, consistent with a high processivity. The fitted red lines are hidden Markov model fits. The absence of any significant short-lived FRET state excursions suggests the scarcity of random Brownian rotation events, at least over the time course of the experiment.

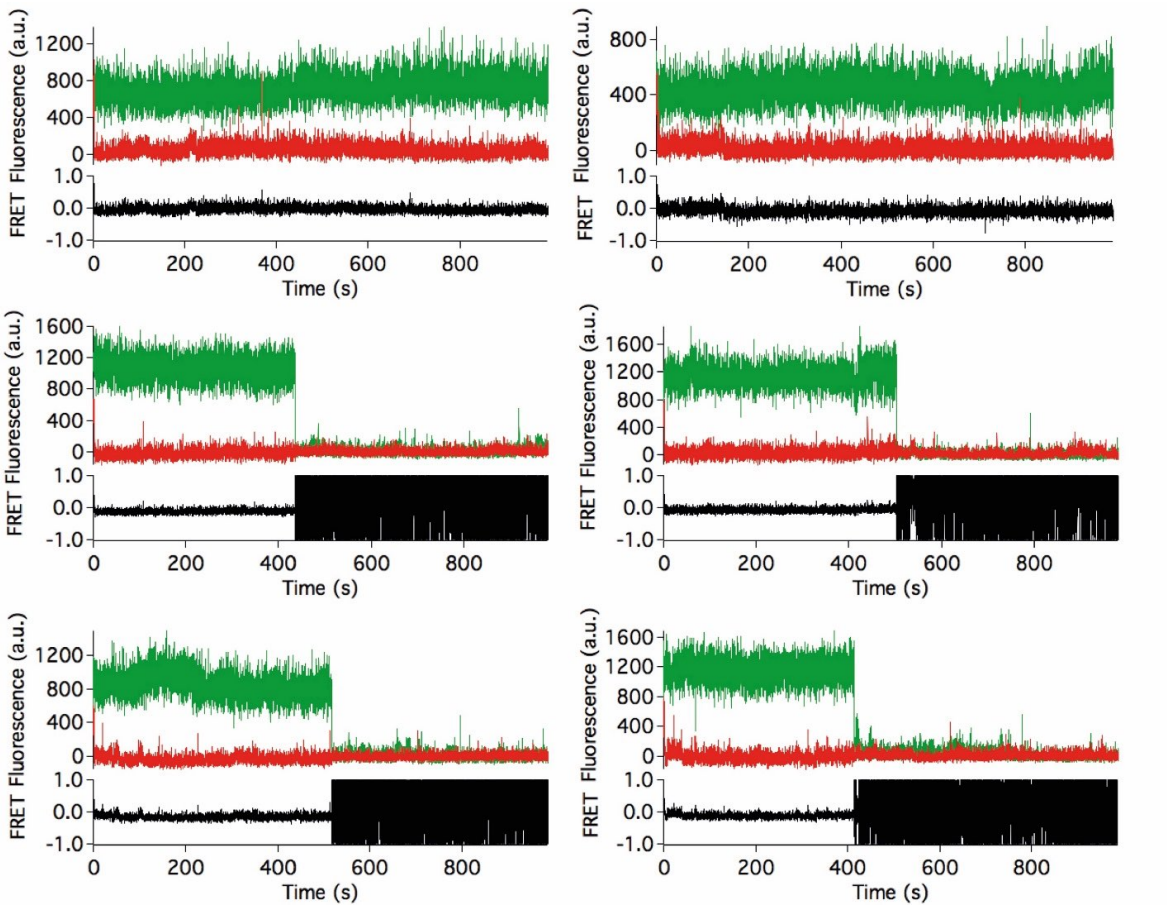

Supplementary Fig. 10. Representative donor (green), acceptor (red) and FRET (black) signal in trajectories from the T7RNAP control experiment for the 126-bp rotor. The brief, high-intensity red signals at the very beginning of each trajectory reflect direct excitation of Cy5, confirming its presence on the stator; the sudden loss of donor signal in the third to sixth trace reflects single-step photobleaching, as expected for a single molecule fluorescence experiment.

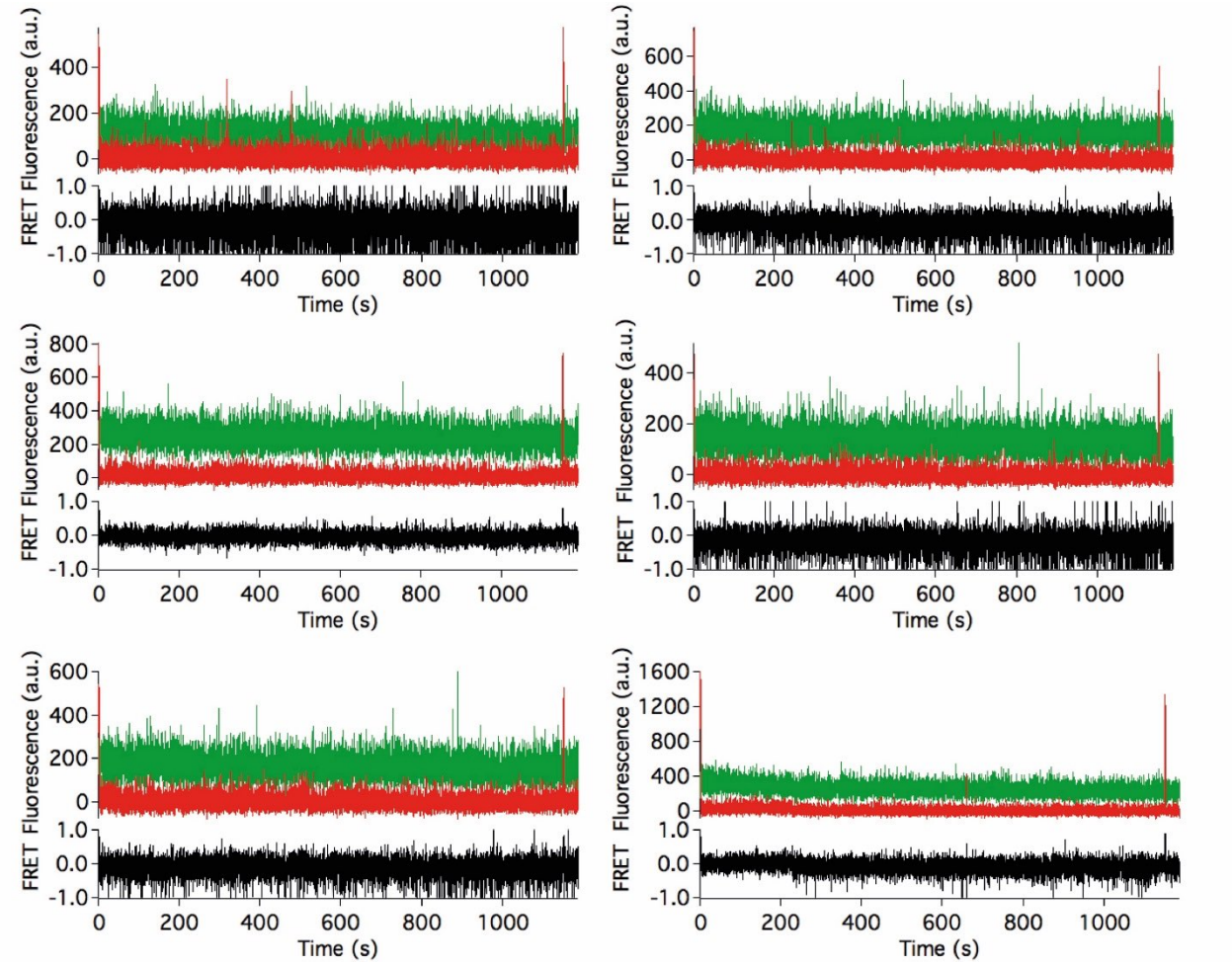

Supplementary Fig. 11. Representative smFRET trajectories from the T7RNAP-ZIF control experiment without NTPs for the 210-bp rotor. The brief, high-intensity red signals at the very beginning and toward the end of each trajectory reflect direct excitation of Cy5, confirming its presence on the stator.

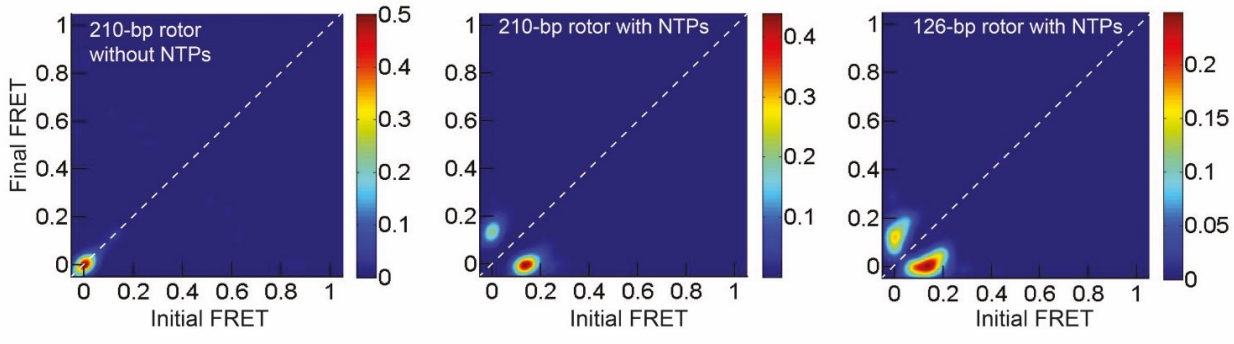

Supplementary Fig. 12. Transition occupation density plots (TODP) for the 210- and 126-bp rotors. The population on the diagonal represents the fraction of static rotors, whereas off-diagonal peaks represent rotors dynamically transitioning between defined FRET states during the observation time windows of individual smFRET trajectories.

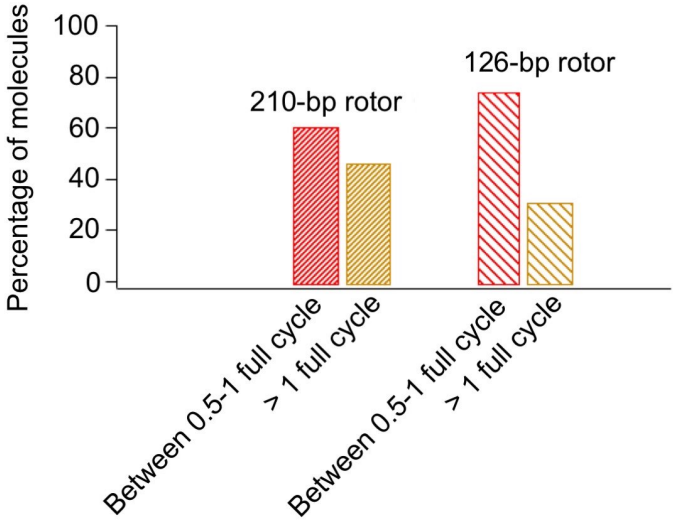

Supplementary Fig. 13. Percentage of single 210- and 126-bp rotor nanoengines exhibiting either partial or more than full transcription cycles within the ~20 min observation time window.

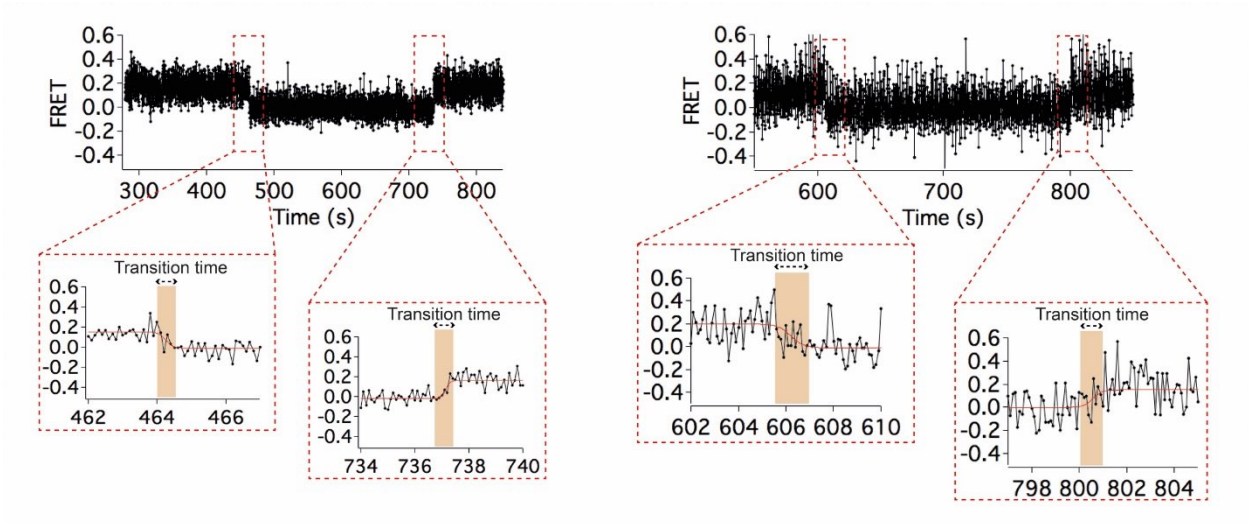

Supplementary Fig. 14. Single molecule FRET trajectories highlighting FRET transitions between high- and low-FRET states. The zoomed insets highlight the gradual changes in FRET value during the transitions from one state to another and their symmetric features.

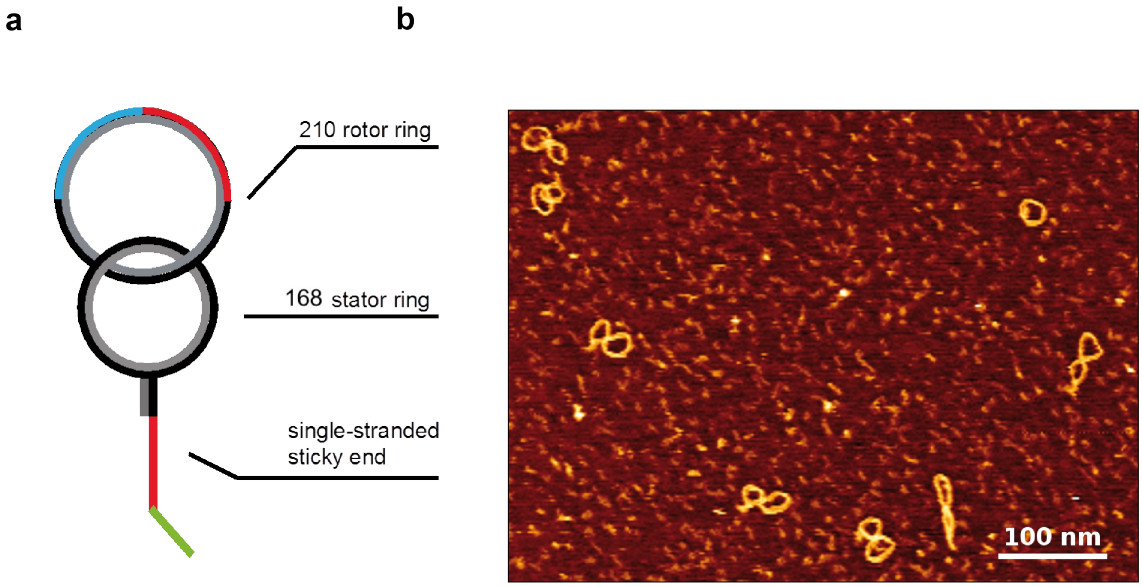

Supplementary Fig. 15. Design and AFM analysis of the catenane walker. (**a**) Scheme of the DNA catenane walker bearing a single stranded sticky end for the specific hybridization to Step1 or Step2 on a predefined DNA path. (**b**) AFM imaging in tapping mode in liquid confirmed the integrity of the DNA catenane walker having a 210-bp ring as rotor.

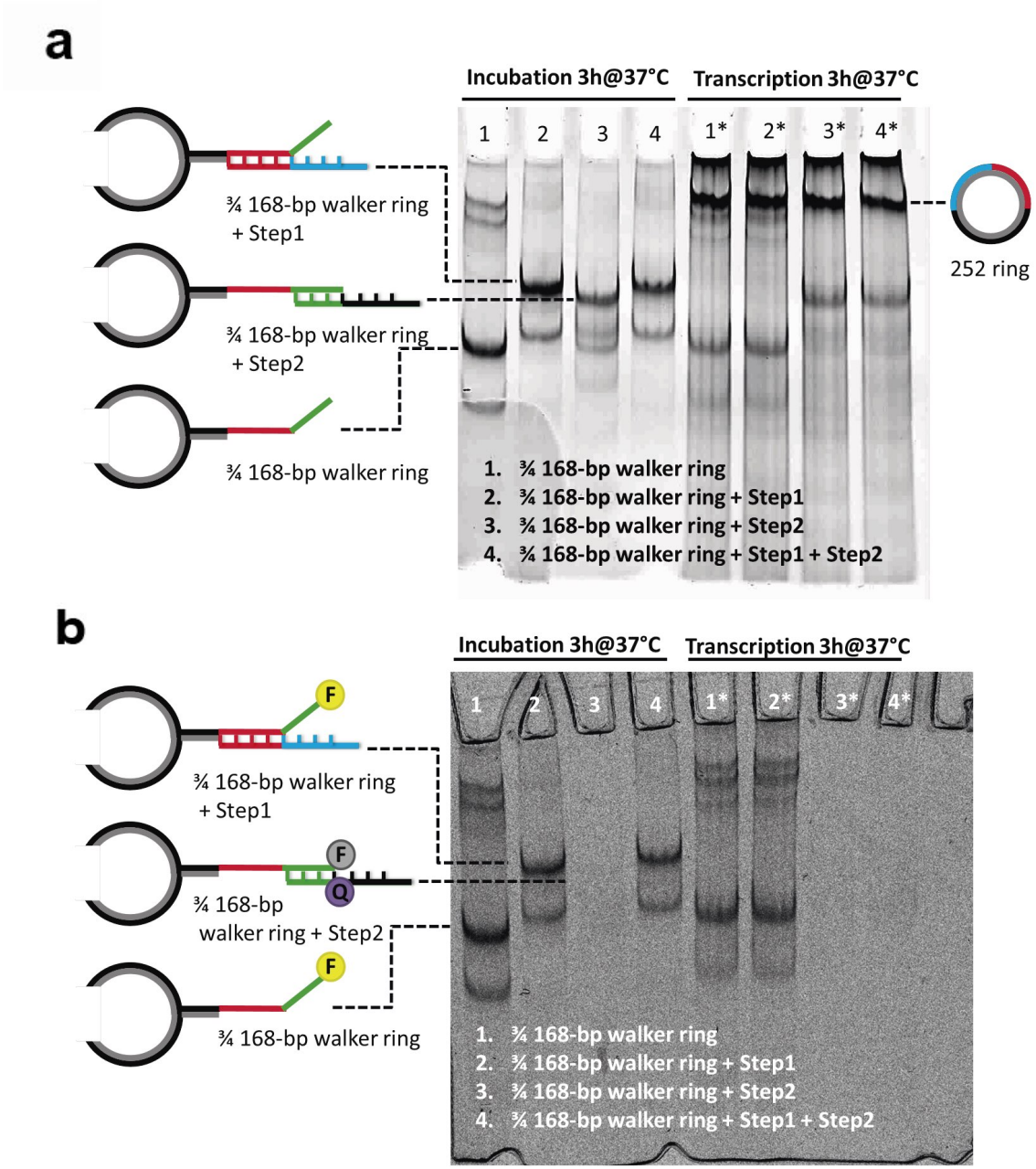

Supplementary Fig. 16. Gel electrophoretic analysis showing selective binding of the 3/4 168-bp walker ring to Steps 1 and 2. (**a**) Lane 1: Unpurified ¾ 168-bp walker ring. Lane 2. Walker ring hybridized to Step1. Lane 3: Walker ring hybridized to Step 2. Lane 4: Walker ring in the presence of both steps, showing selective binding to Step1. Lanes 1-4*. Same sample composition as their corresponding analog lane in which transcription with a 252-bp ring (analog to the 126-bp rotor) has taken place for 3 h. As observed, ring walker is efficiently displaced from Step 1 to Step 2 upon transcription, remaining bound to the last (lane 4*). (**b**) Fluorescence-Electrophoretic Gel Shift Assay (F-EMSA) performed prior ethidium bromide staining. Fluorophore-quencher pairs described in Figure 3 were used to track the different hybridization species. Upon hybridization to Step2 which contains BHQ-2, the band corresponding with the walker ring (fluorescently labelled with TAMRA) is not detectable.

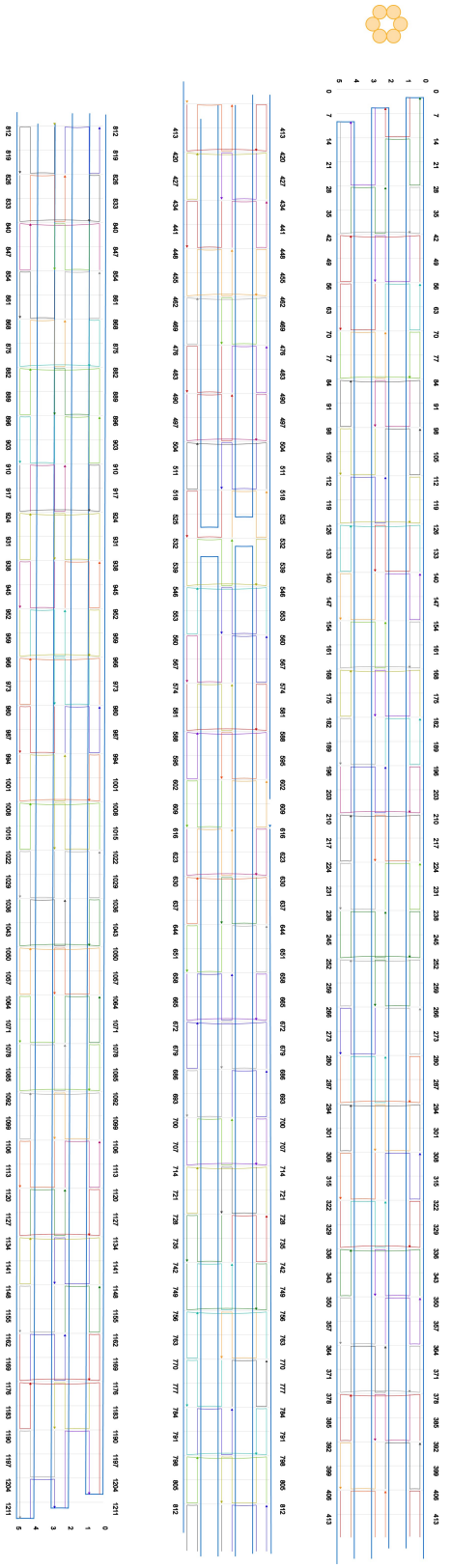

Supplementary Fig. 17. Detailed scheme of the six-helix bundle DNA origami designed using caDNAno[3]. Modified ODNs used for the assembly of the different 6HB DNA origami paths. **Three iSteps path (Qdot attachment)**: Substitute

6HB_JV34, 6HB_JV92, 6HB_JV95, 6HB_JV104 and 6HB_JV51 for Step1_6HB_JV34, iSteplong2_6HB_JV92, iSteplong4_6HB_JV95, iSteplong7_6HB_JV104 and Step2b_6HB_JV51. **Three iSteps path (fluorescence):** Substitute 6HB_JV34, 6HB_JV92, 6HB_JV95, 6HB_JV104 and 6HB_JV51 for Step1_6HB_JV34, iSteplong2_6HB_JV92(HEX), iSteplong4_6HB_JV95, iSteplong7_6HB_JV104(TxR) and Step2b_6HB_JV51. **Three iSteps path (fluorescence control):** Substitute 6HB_JV34, 6HB_JV92, 6HB_JV95, 6HB_JV104 and 6HB_JV51 for Step1_6HB_JV34, iSteplong2_6HB_JV92, iSteplong5_6HB_JV98(FAM), iSteplong7_6HB_JV104(TxR) and Step2b_6HB_JV51. **Path A:** Substitute 6HB_JV34, 6HB_JV95 and 6HB_JV40 for Step1_6HB_JV34, iSteplong4_6HB_JV95 and Step2b_6HB_JV40. **Path B:** Substitute 6HB_JV34, 6HB_JV95 and 6HB_JV51 for Step1_6HB_JV34, iSteplong4_6HB_JV95 and Step2b_6HB_JV51. **Path C:** Substitute 6HB_JV34, 6HB_JV92 and 6HB_JV51 for Step1_6HB_JV34, iSteplong2_6HB_JV92 and Step2b_6HB_JV51. **Path D:** Substitute 6HB_JV34, 6HB_JV107 and 6HB_JV51 for Step1_6HB_JV34, iSteplong8_6HB_JV107 and Step2b_6HB_JV51. **Path ΔC:** Substitute 6HB_JV34 and 6HB_JV92 for Step1_6HB_JV34, and iSteplong2_6HB_JV92. **Path ΔD:** Substitute 6HB_JV34 and 6HB_JV107 for Step1_6HB_JV34 and iSteplong8_6HB_JV107.

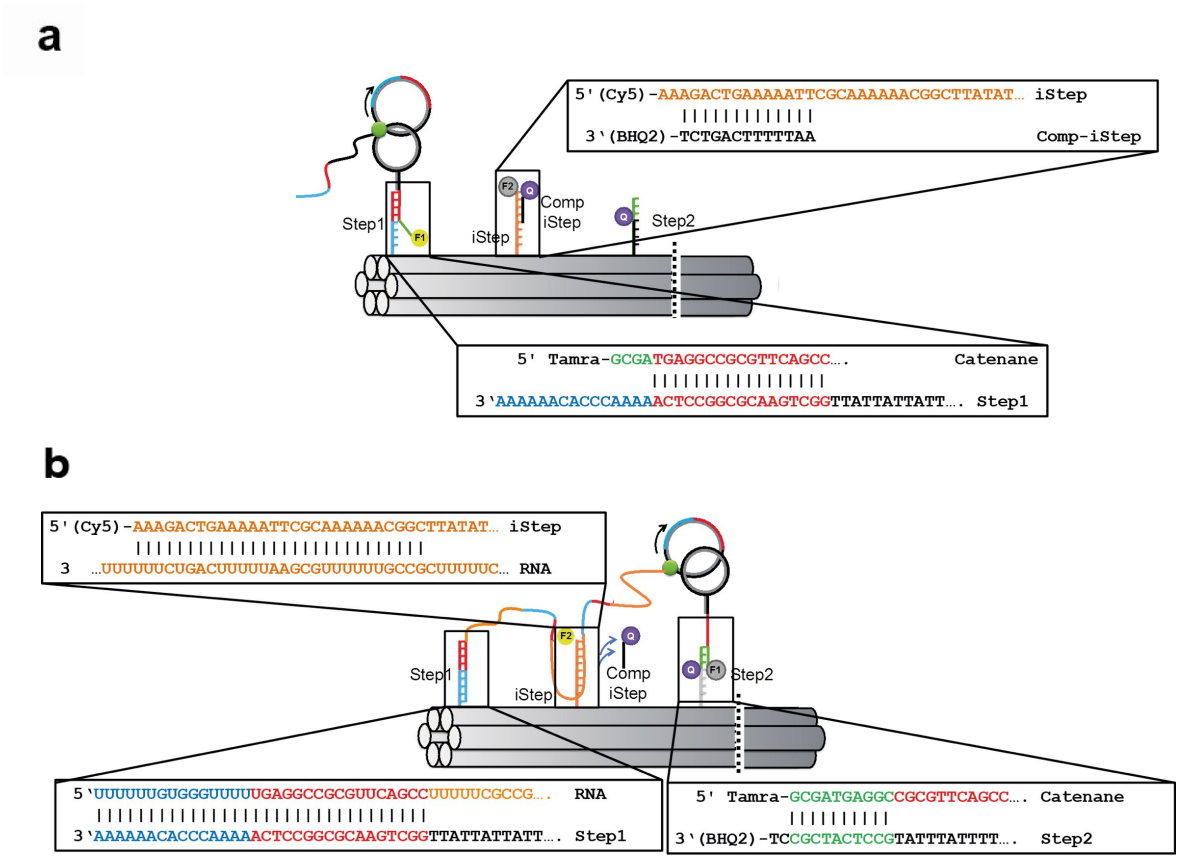

Supplementary Fig. 18. Detailed scheme of the working principle of the DNA catenane walker, showing the specific sequences involved in the hybridization and strand-displacement reactions occurring before (**a**) and after (**b**) transcription. F1: TAMRA; F2: Cy5; Q Black hole quencher 2 (BHQ2). Green circle: T7RNAP-ZIF.

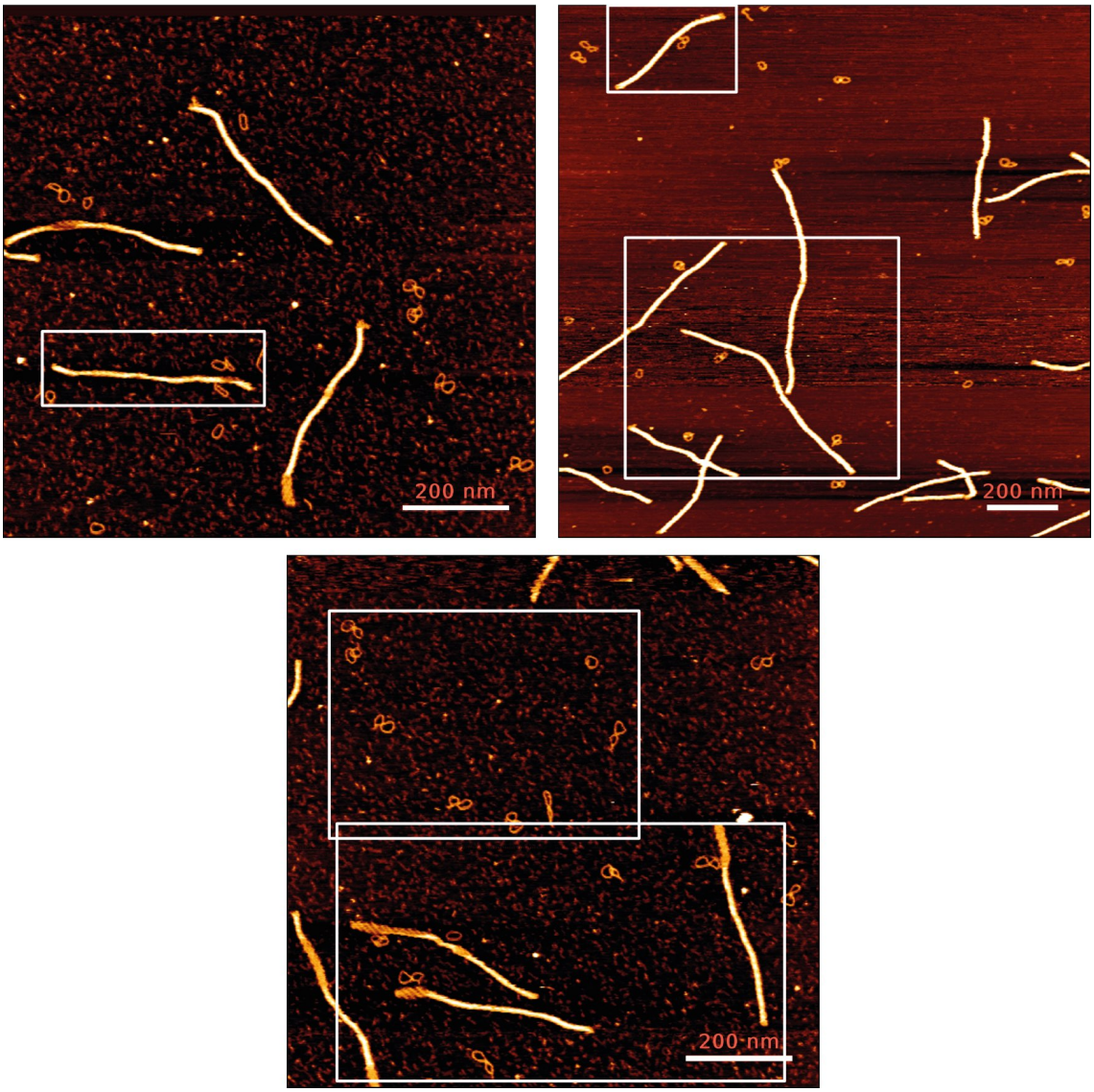

Supplementary Fig. 19. Larger sections from the uncropped AFM images used for the panels in Figure 3f,g and Suppl. Fig. 15b.

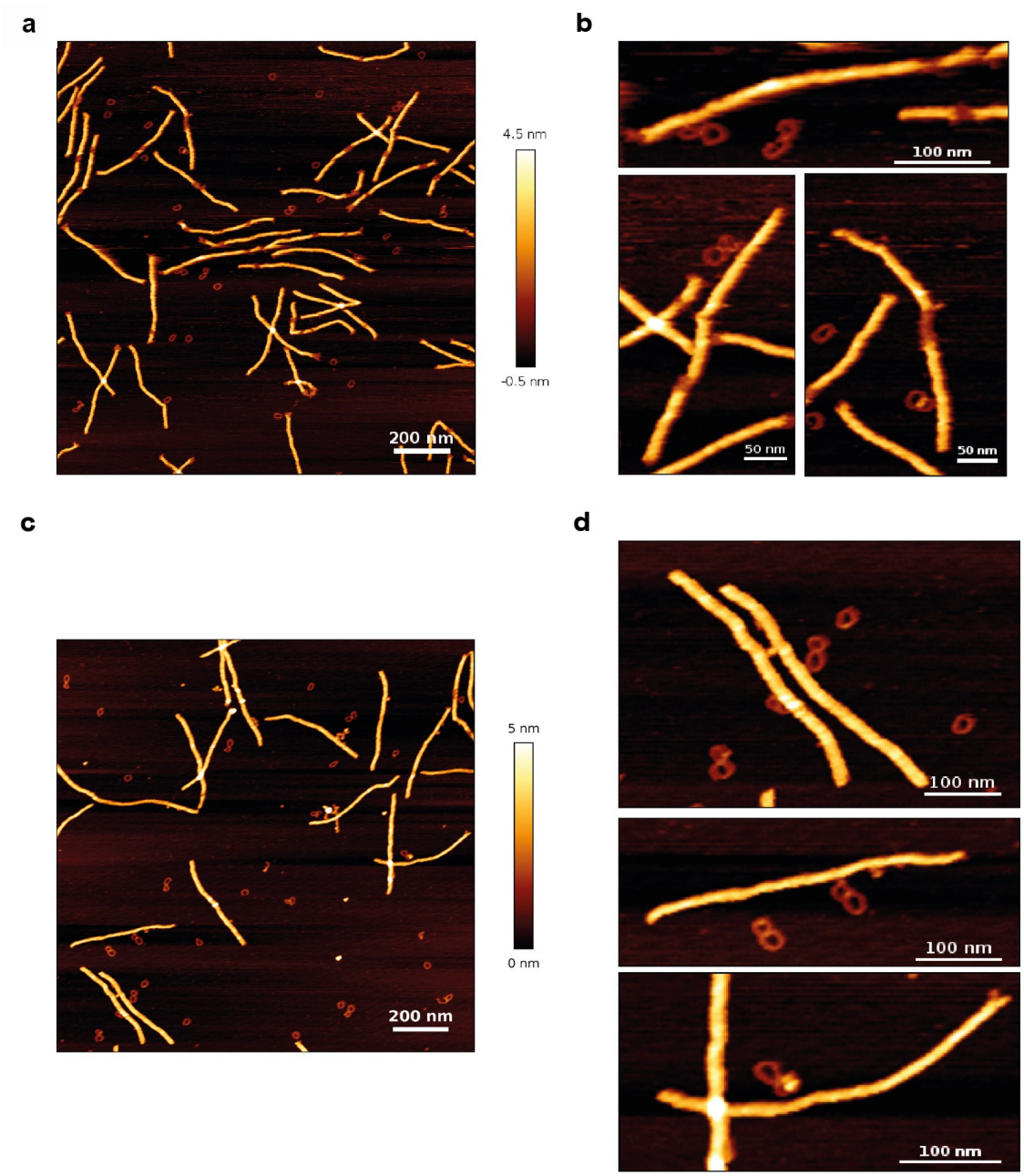

Supplementary Fig. 20. Tapping mode AFM imaging in liquid of the catenane nanoengine together with the DNA path before and after transcription. (**a**) AFM imaging of the catenane nanoengine before transcription in the presence of the DNA origami path. Despite AFM conditions were not optimal for hybridization, all assembled structures, i.e. where the catenane is interacting with the DNA origami path, show the catenane positioned in Step1. (**b**) Detailed pictures of catenane nanoengines before transcription assembled to the Step1 position of the DNA path. (**c**) AFM imaging of the catenane nanoengine after transcription in the presence of the DNA origami path. All assembled structures, i.e. where the catenane is interacting with the DNA origami path, show the catenane positioned in Step2. (**d**) Detailed pictures of catenane nanoengines after transcription assembled to the Step2 position of the DNA path.

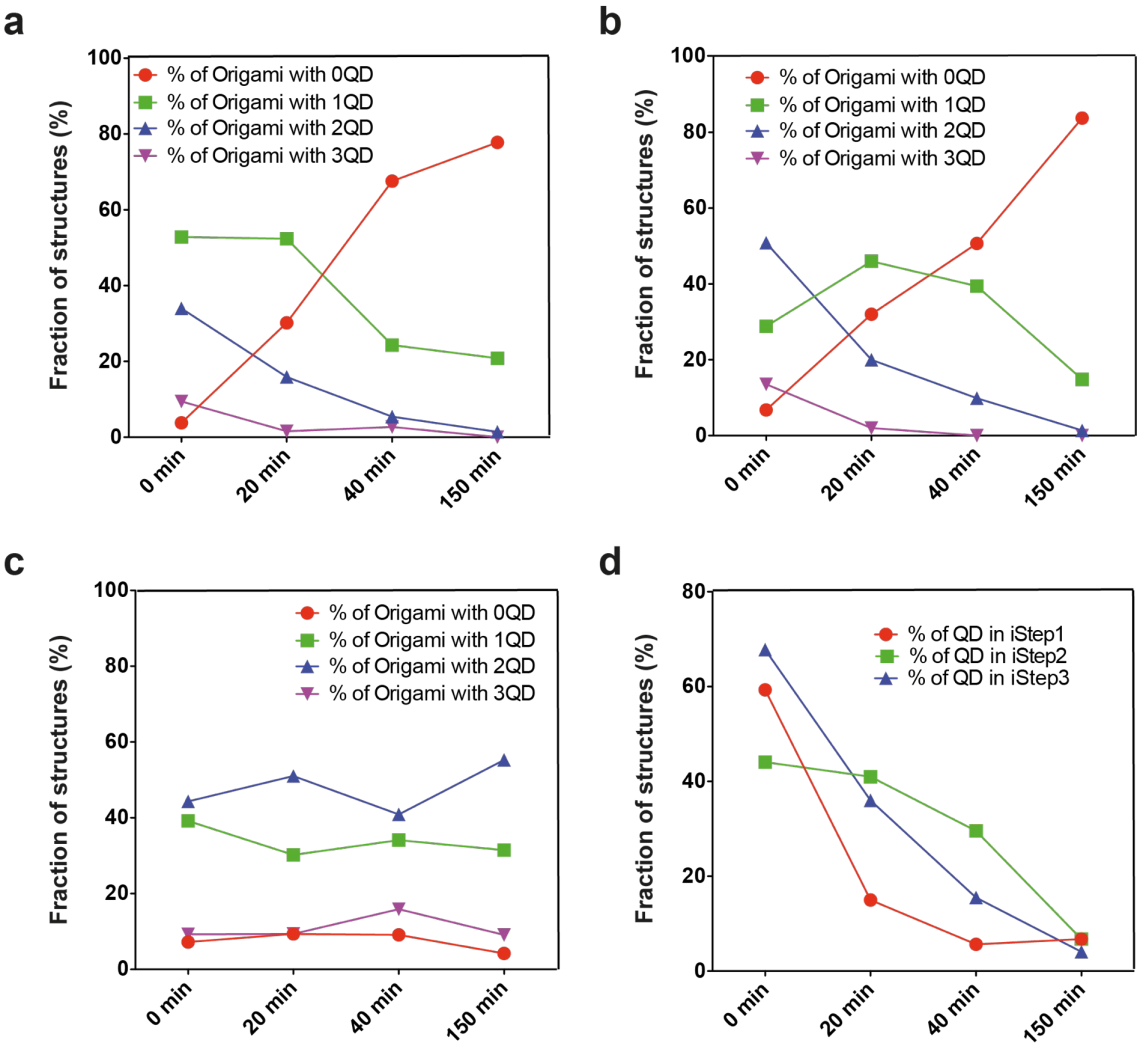

Supplementary Fig. 21. Qdot attachment upon transcription by AFM analysis (**a-c**) Fraction of structures found by AFM analysis with diverse number of Qdots at different time points in the presence of the catenane walker with the 210-bp rotor ring (**a**), the 126-bp rotor ring (**b**) and in absence of catenane walker (**c**, non transcription control). (**d**) Qdot occupancy for each origami position at different time points in presence of the catenane walker containing the 126-bp rotor ring (iStep1 [red], iStep2 [green], iStep3 [blue]).

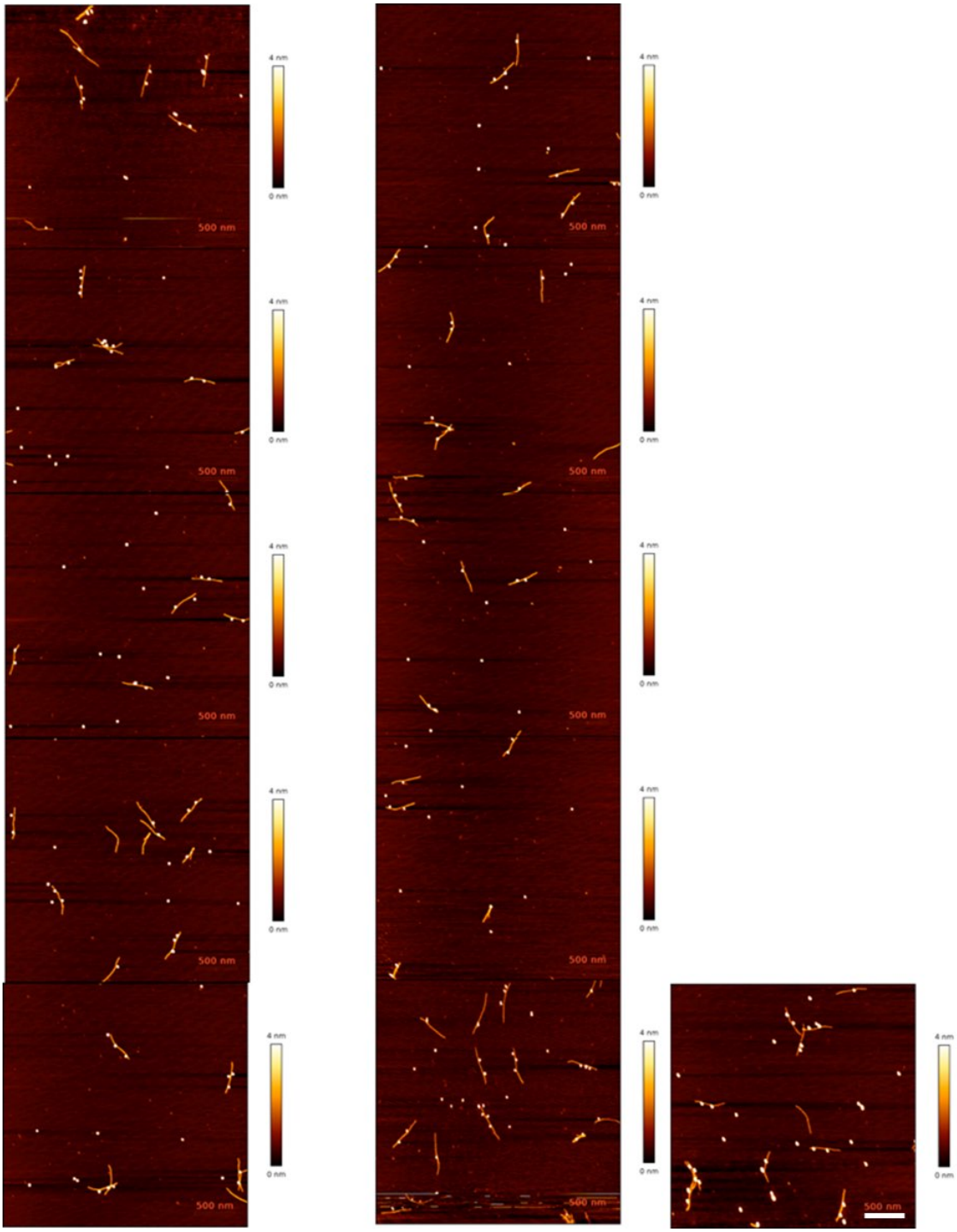

Supplementary Fig. 22. AFM images corresponding with the Qdot tagging of the bio-comp-iSteps on the DNA origami path upon transcription with Catenane walker (210-bp rotor). Time 0 min. The scans reflect a continuous surface, but images were measured subsequently and then re-aligned.

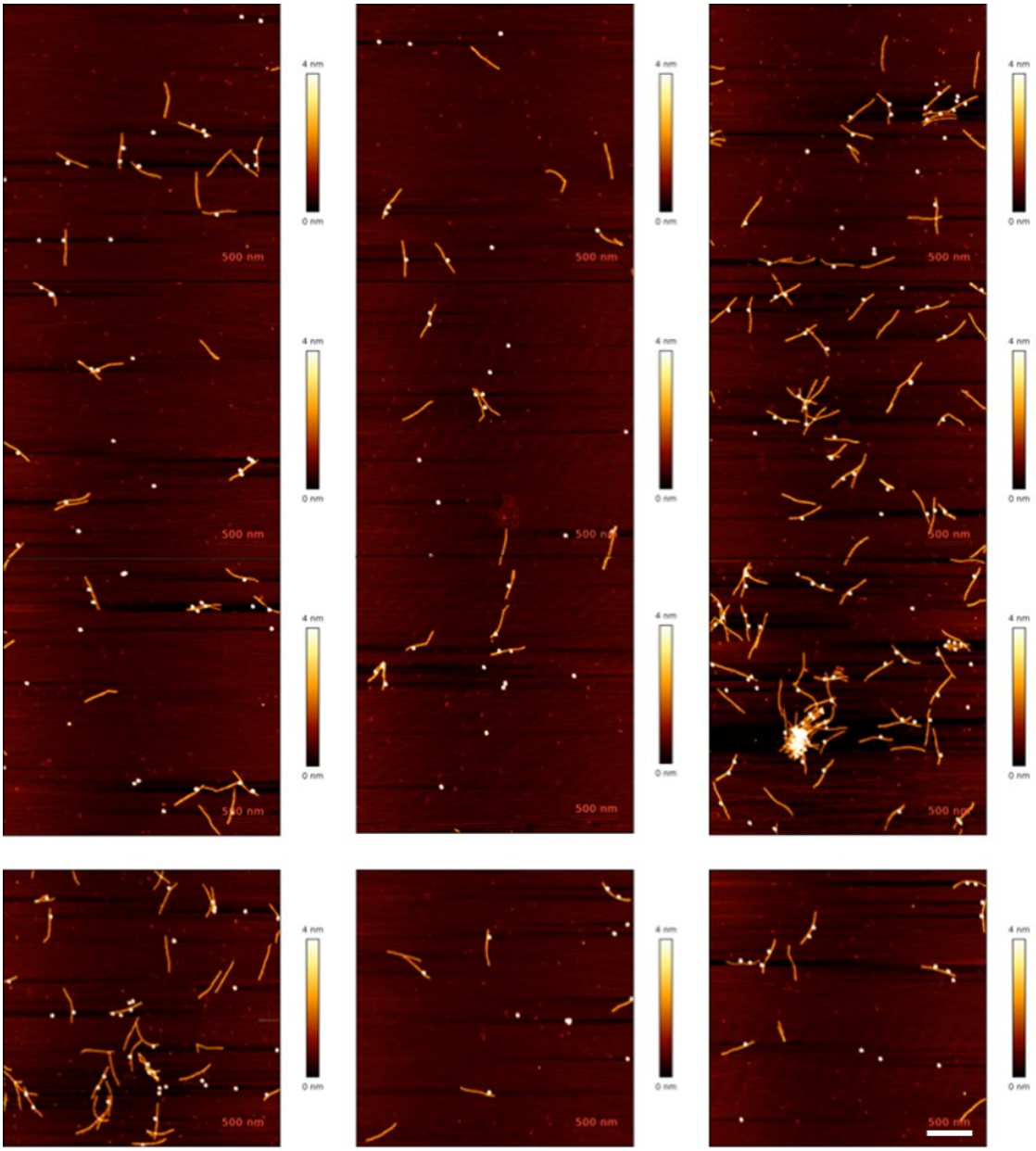

Supplementary Fig. 23. AFM images corresponding with the Qdot tagging of the bio-comp-iSteps on the DNA origami path upon transcription with Catenane walker (210-bp rotor). Time 20 min. The scans reflect a continuous surface, but images were measured subsequently and then re-aligned.

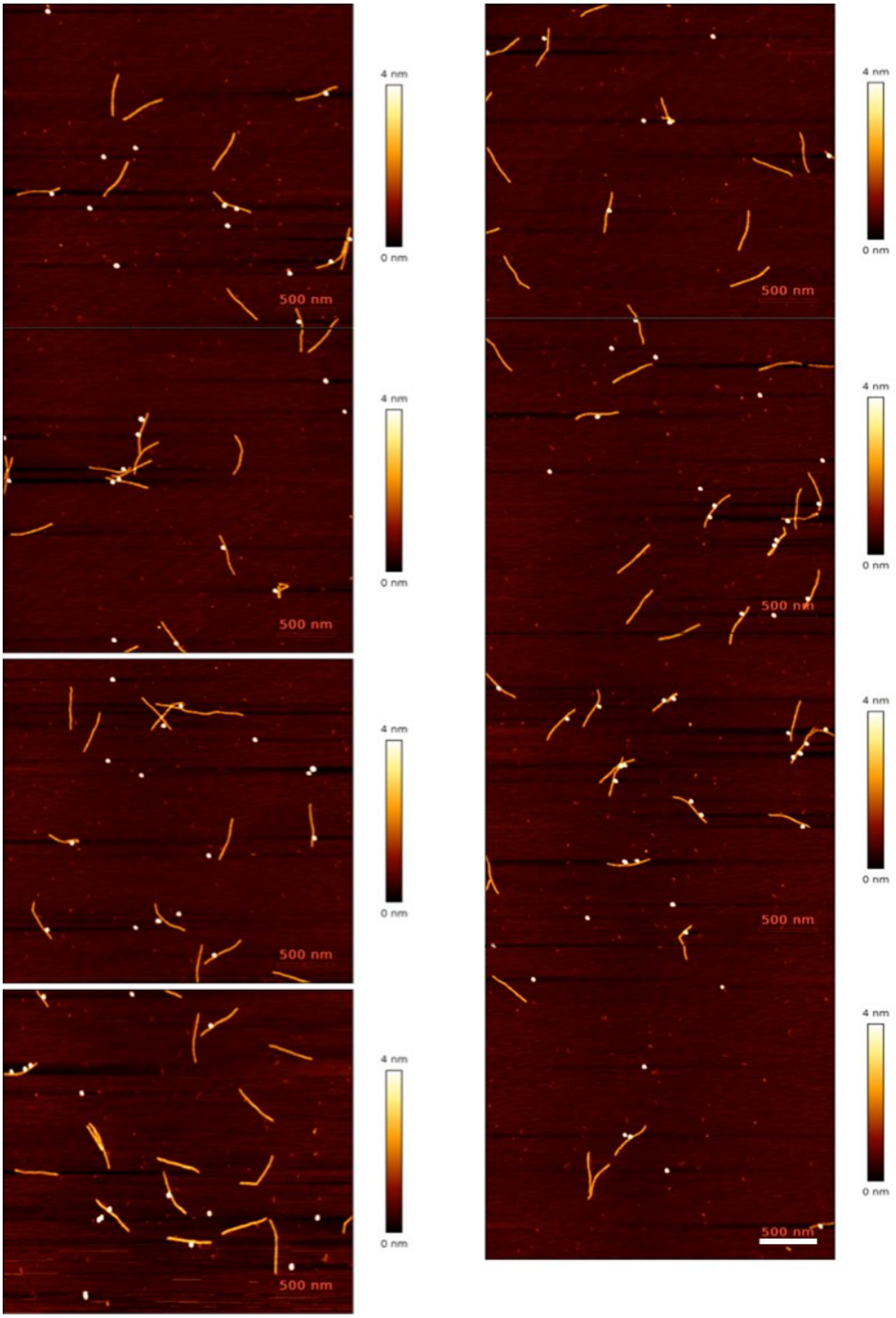

Supplementary Fig. 24. AFM images corresponding with the Qdot tagging of the bio-comp-iSteps on the DNA origami path upon transcription with Catenane walker (210-bp rotor). Time 40 min. The scans reflect a continuous surface, but images were measured subsequently and then re-aligned.

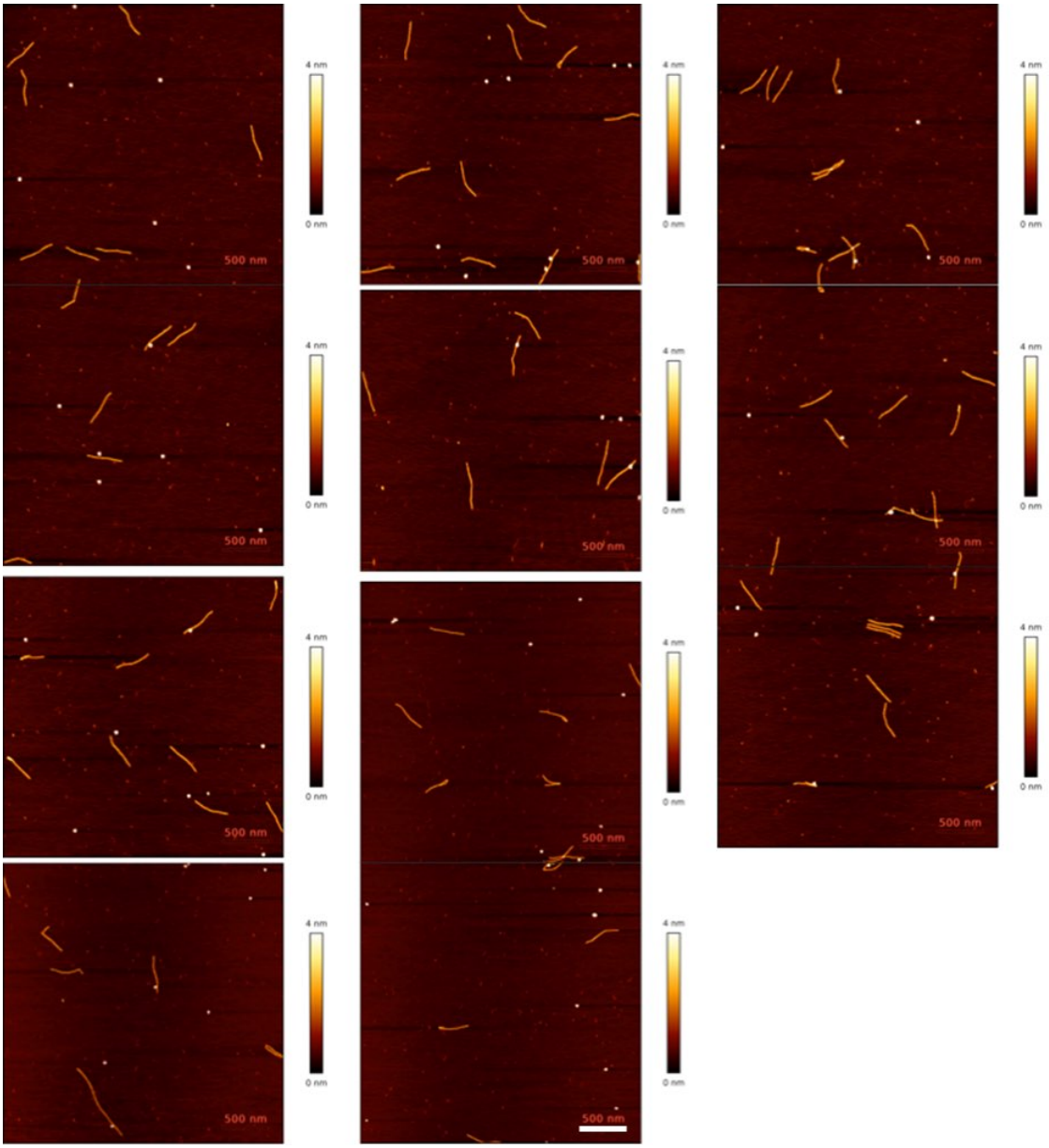

Supplementary Fig. 25. AFM images corresponding with the Qdot tagging of the bio-comp-iSteps on the DNA origami path upon transcription with Catenane walker (210-bp rotor). Time 150 min. The scans reflect a continuous surface, but images were measured subsequently and then re-aligned.

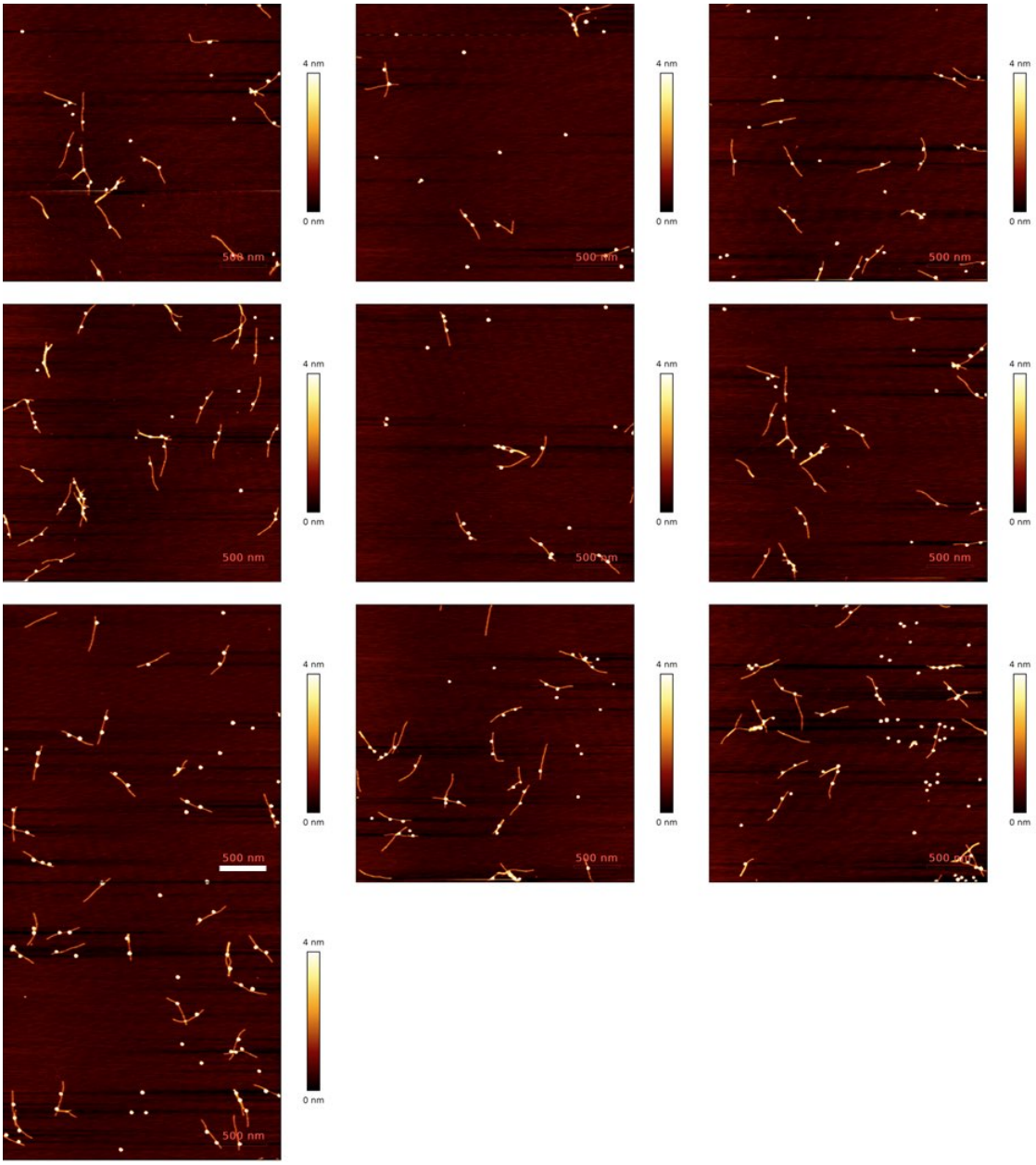

Supplementary Fig. 26. AFM images corresponding with the Qdot tagging of the bio-comp-iSteps on the DNA origami path for the no transcription control. Time 0 min. The scans reflect a continuous surface, but images were measured subsequently and then re-aligned.

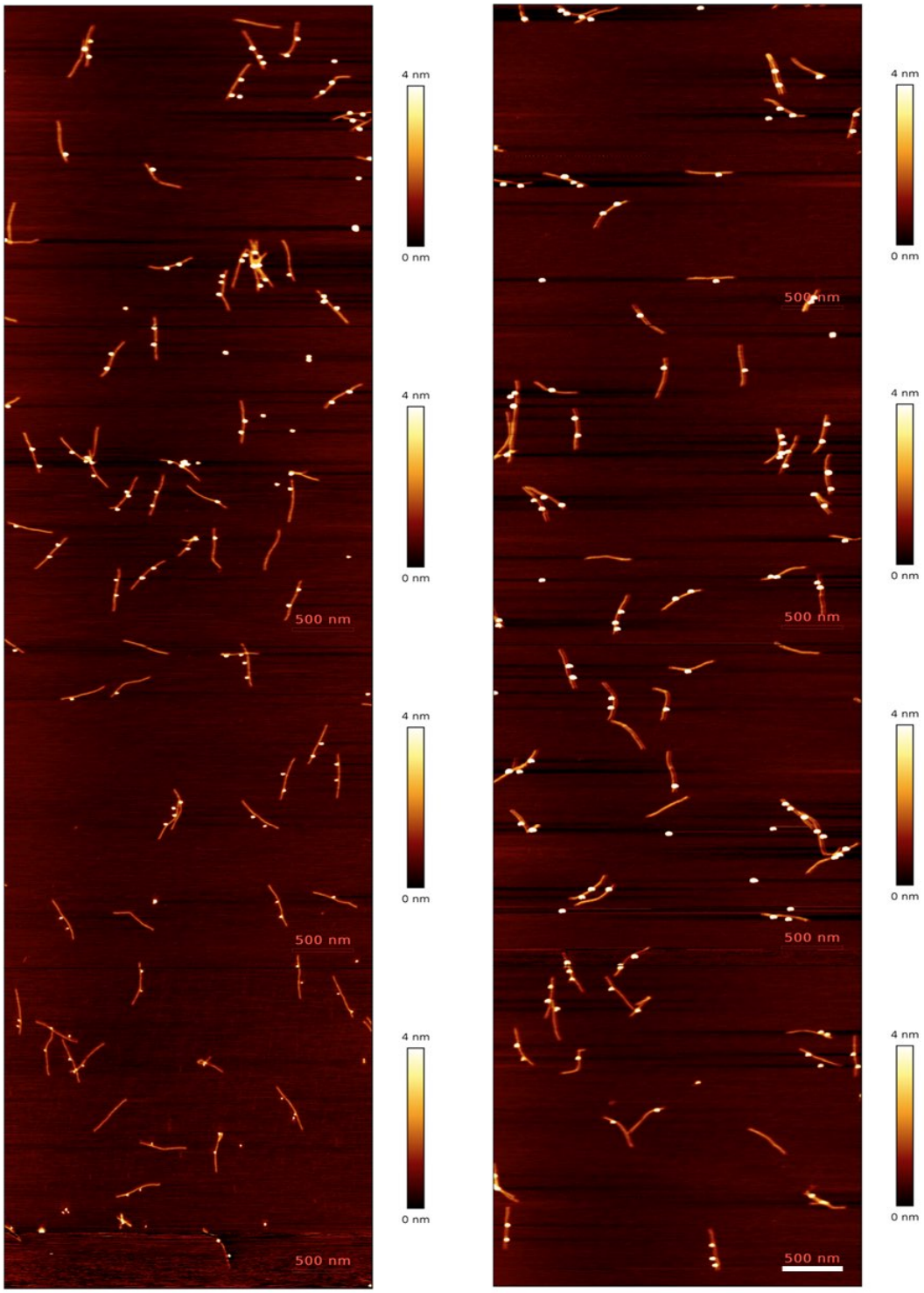

Supplementary Fig. 27. AFM images corresponding with the Qdot tagging of the bio-comp-iSteps on the DNA origami path for the no transcription control. Time 20 min. The scans reflect a continuous surface, but images were measured subsequently and then re-aligned.

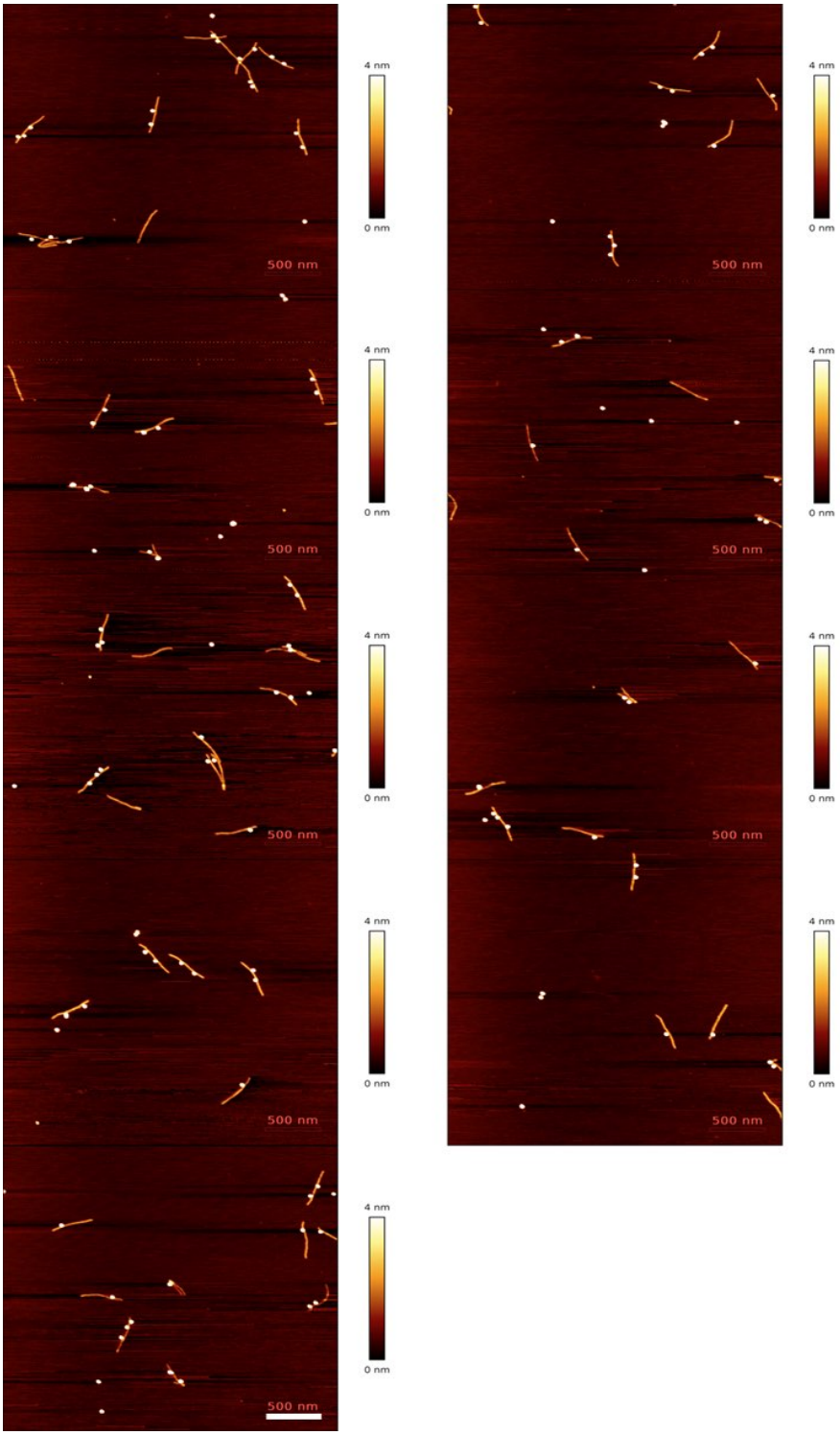

Supplementary Fig. 28. AFM images corresponding with the Qdot tagging of the bio-comp-iSteps on the DNA origami path for the no transcription control. Time 40 min. The scans reflect a continuous surface, but images were measured subsequently and then re-aligned.

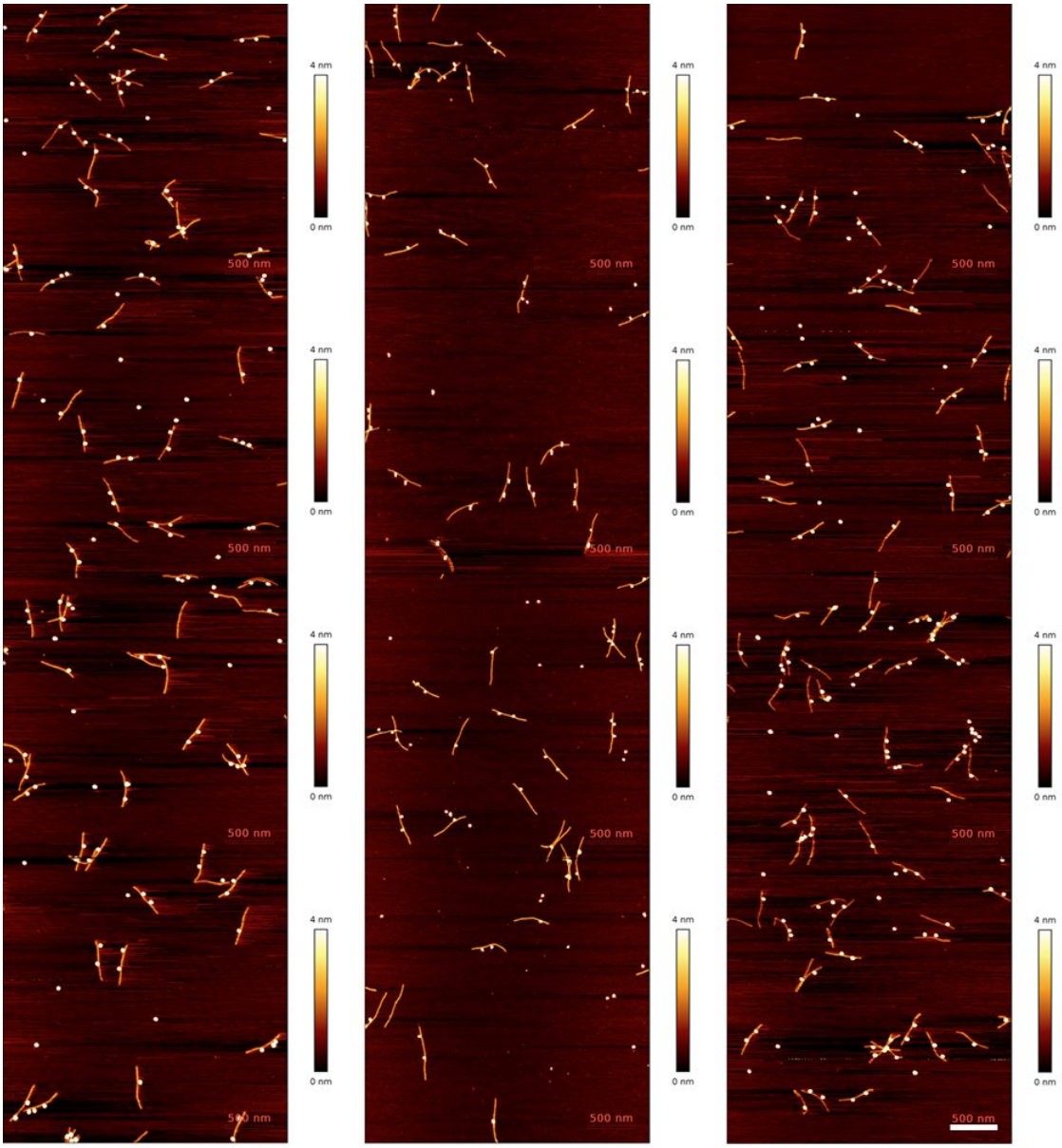

Supplementary Fig. 29. AFM images corresponding with the Qdot tagging of the bio-comp-iSteps on the DNA origami path for the no transcription control. Time 150 min. The scans reflect a continuous surface, but images were measured subsequently and then re-aligned.

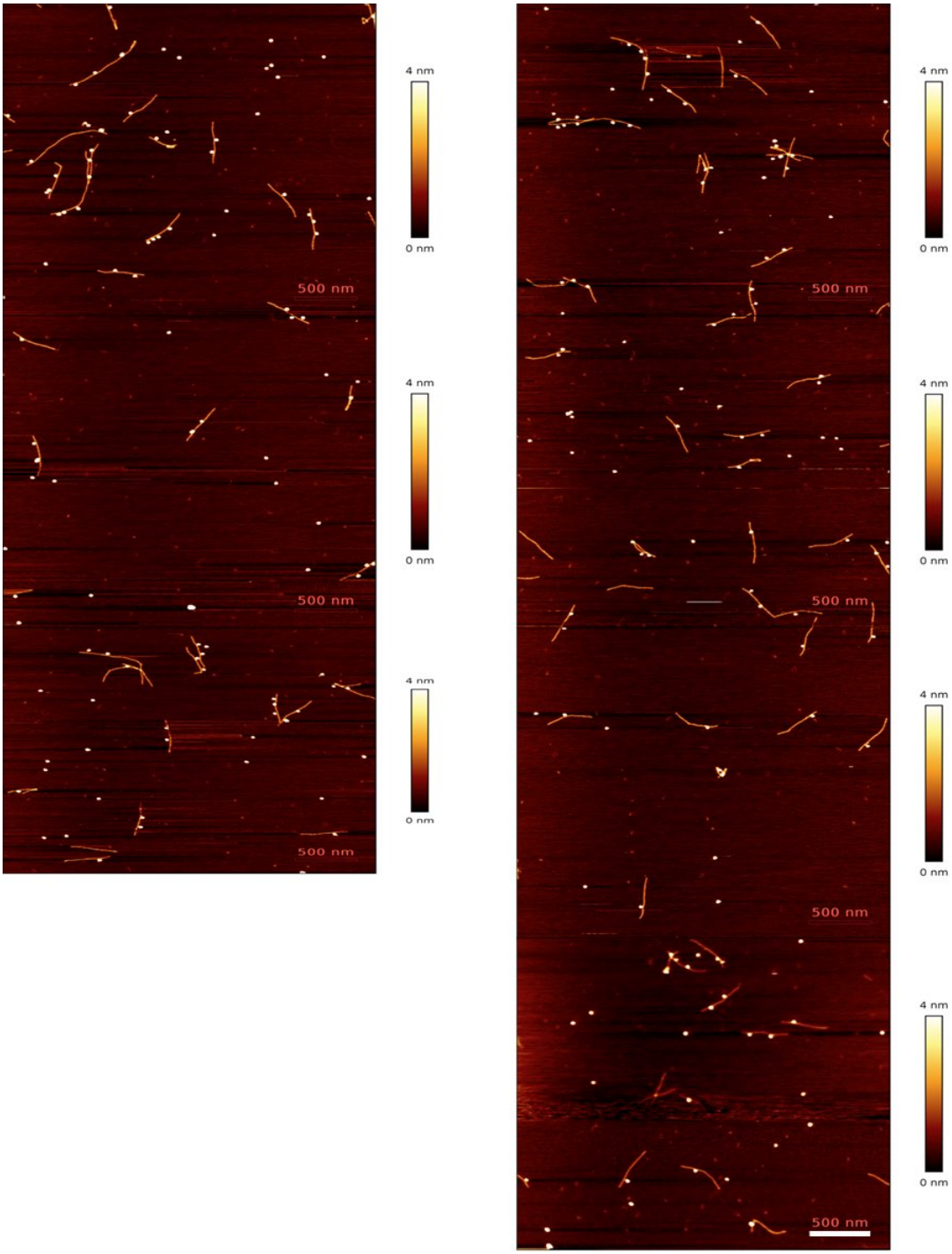

Supplementary Fig. 30. AFM images corresponding with the Qdot tagging of the bio-comp-iSteps on the DNA origami path upon transcription with Catenane walker (126-bp rotor). Time 0 min. The scans reflect a continuous surface, but images were measured subsequently and then re-aligned.

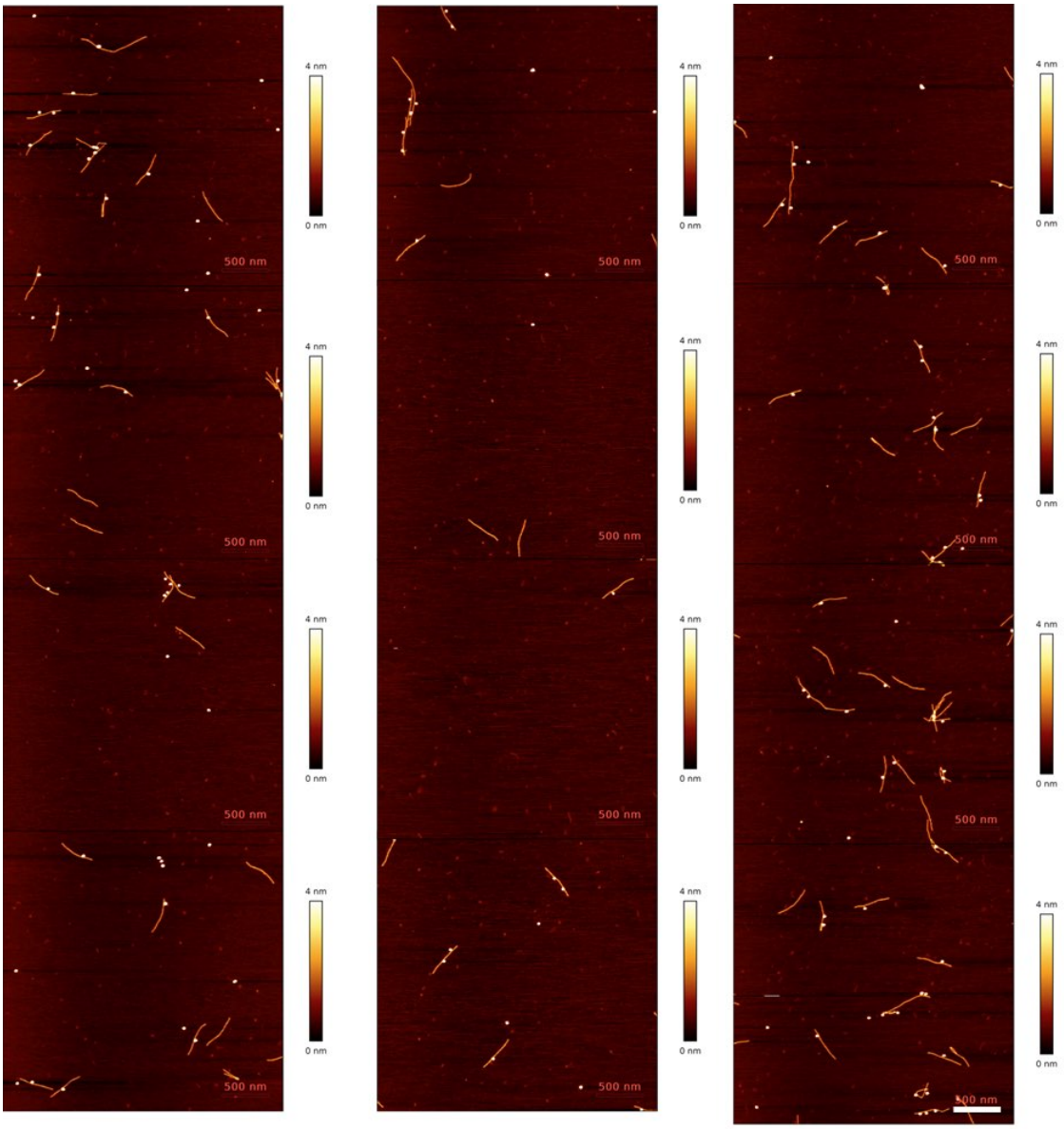

Supplementary Fig. 31. AFM images corresponding with the Qdot tagging of the bio-comp-iSteps on the DNA origami path upon transcription with Catenane walker (126-bp rotor). Time 20 min. The scans reflect a continuous surface, but images were measured subsequently and then re-aligned.

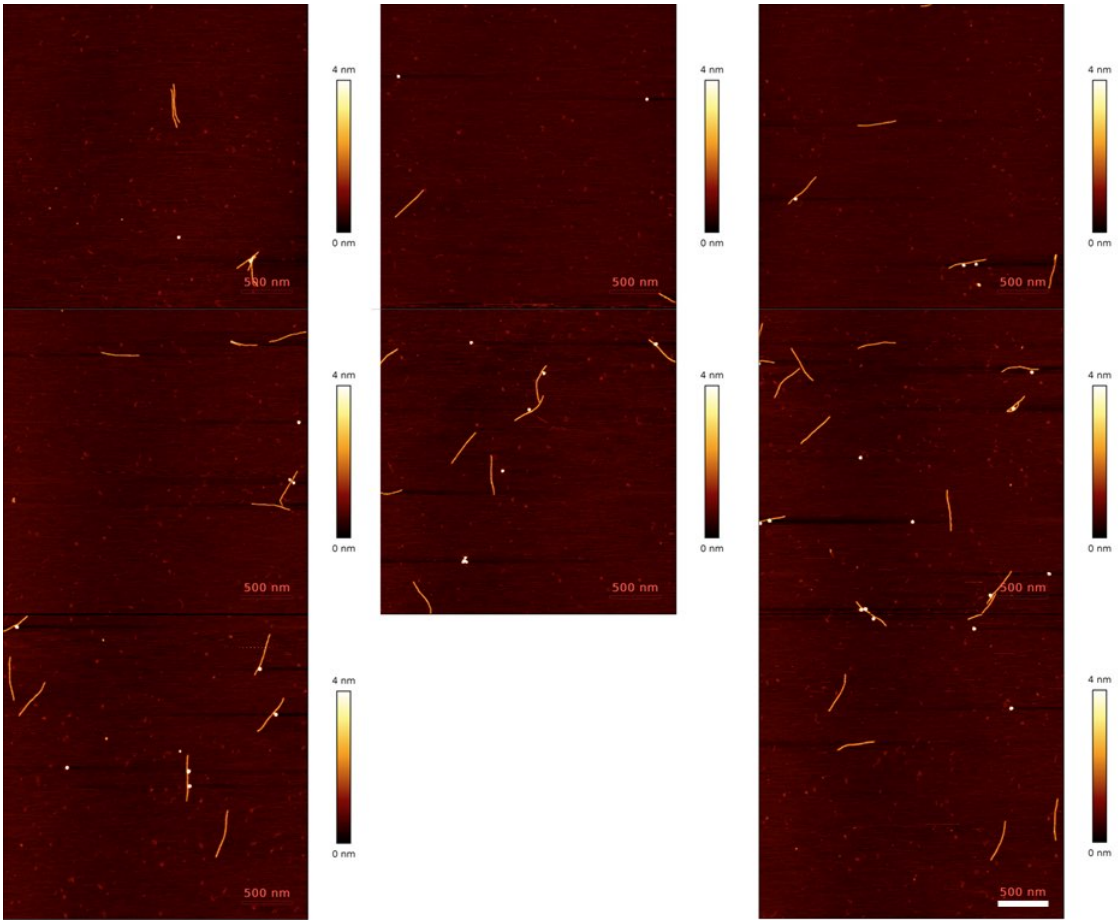

Supplementary Fig. 32. AFM images corresponding with the Qdot tagging of the bio-comp-iSteps on the DNA origami path upon transcription with Catenane walker (126-bp rotor). Time 40 min. The scans reflect a continuous surface, but images were measured subsequently and then re-aligned.

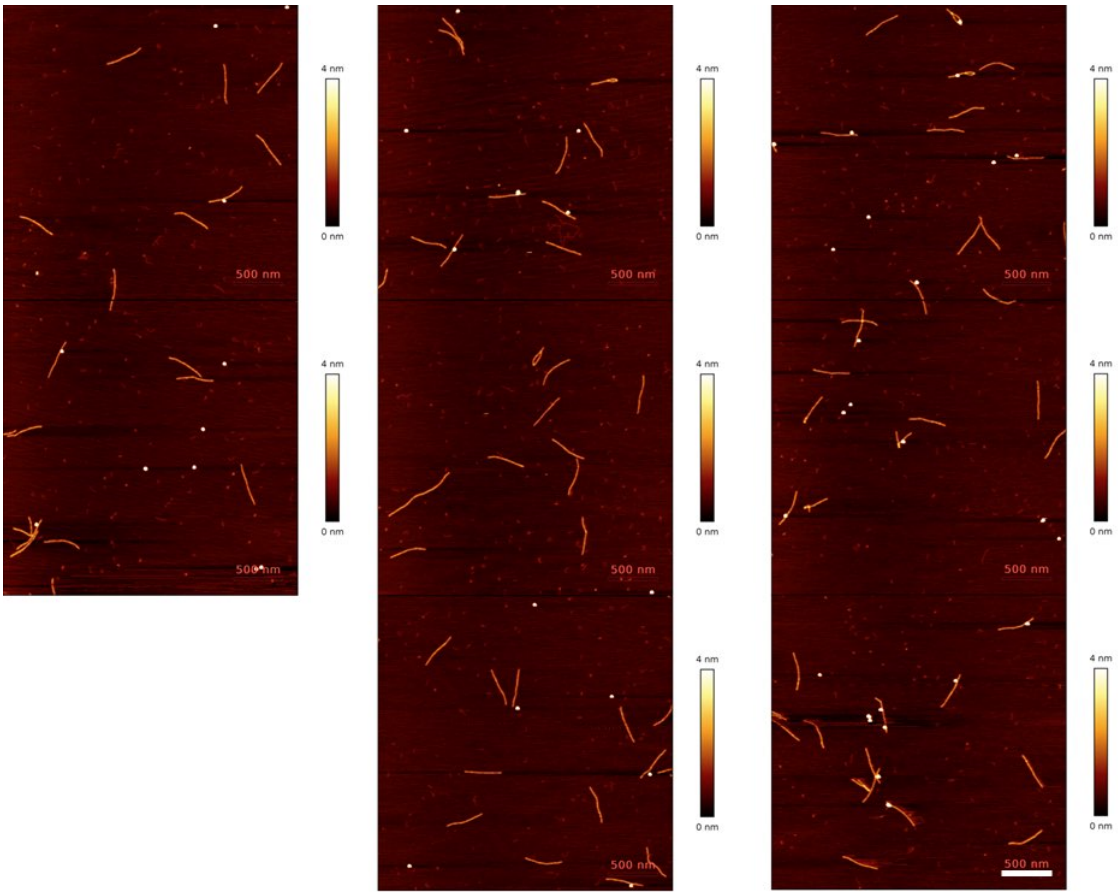

Supplementary Fig. 33. AFM images corresponding with the Qdot tagging of the bio-comp-iSteps on the DNA origami path upon transcription with Catenane walker (126-bp rotor). Time 150 min. The scans reflect a continuous surface, but images were measured subsequently and then re-aligned.

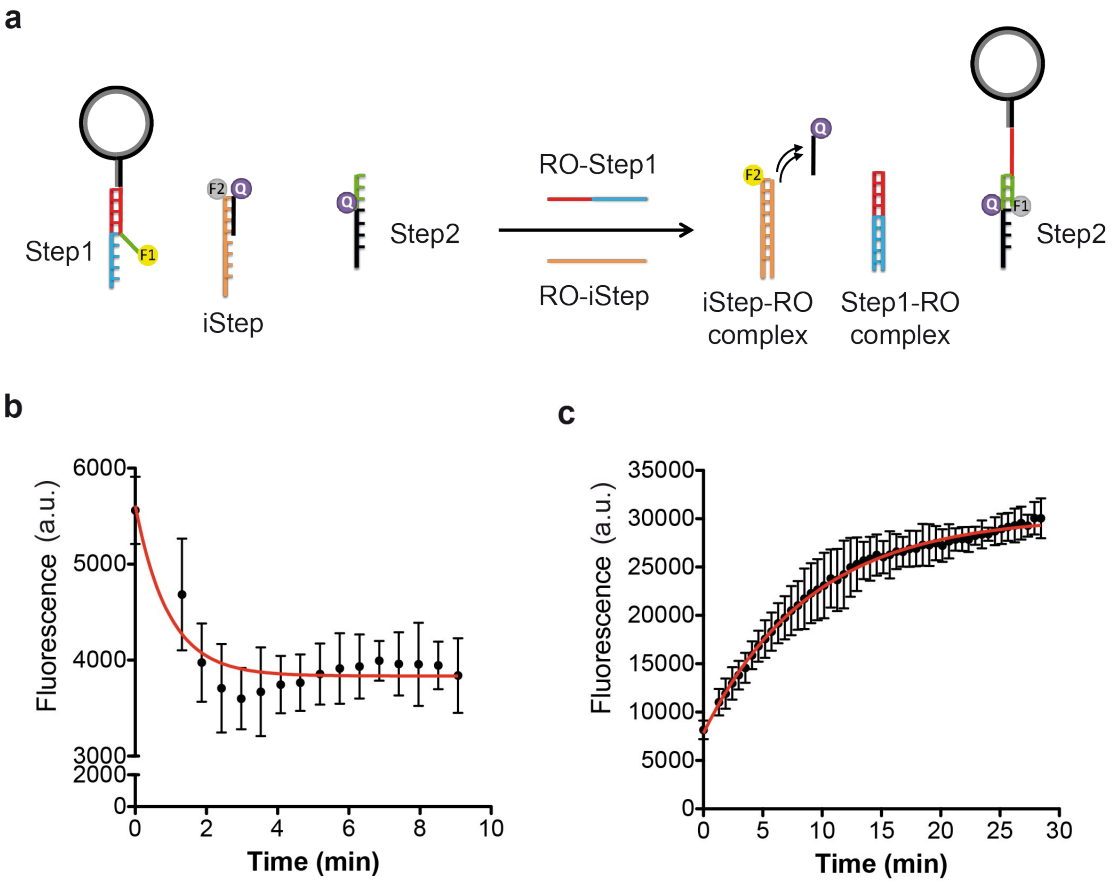

Supplementary Fig. 34. Strand-displacement and hybridization kinetics of the different reactions occurring during catenane walking (**a**) Schematic representation of the assay to measure the strand displacement and hybridization kinetics for Step 1 to 2 translocation of the modified 168bp stator ring and the release of comp-iStep from the iStep by addition of the corresponding release ODNs (RO-Step1 and RO-iStep). (**b** and **c**) Kinetic analysis by exponential fitting of the fluorescence signal resulting from Step 1g2 translocation (**b**) and the release of comp-iStep from the iStep. Error bars: (**c**) by adding RO-Step1 and RO-iStep. Error bars: n = 2, mean ±SD

Supplementary Table 1. List of ODNs used for the assembly of DNA rings and catenanes and origami Steps used in this study.

126-bp rotor ring	
ALGmb_f short	5'phos-AAAGCTGCAAAAAAGACTGAAAAATTCGCAAAA AACGGCGAAAAAGGC
ALgP_f	5'-Phos-AACCCACAAAAAAGTGACAAAAATGCGTAAAAA ATCTCCCTATAGTGAGTCGTATTAATTAA
JVgmblong	5'-Phos-ACTTTTTTGTGGGTTTTTGAGGCCGCGTTCAGCCT TTTTCGCCGTTTTTTGCGAATTTTTCAG
ALgP_r	5'-Phos- TCTTTTTTGCAGCTTTTTAATTAATACGACTCACT ATAGGGAGATTTTTTACGCATTTTTGTC
JVRO2short_f RO_rotor	5'-phosTGAACGCGGCCTCAAA
126-bp control ring (no MB)	
P-mb_r	5'-Phos-AGCTTTTTAATTAATACGACTCACTATAGGGAGA TTTTTTACGCATTTTTGTCACTTTTTTGT
Pt-mb_f	5'-Phos-GACAAAAATGCGTAAAAAATCTCCCTATAGTGA GTCGTATTAATTAAAAAGCTGCAAAAAAGA
nTh_f	5'-Phos-CCCAAAAAGACACAAAAAACGGCGAAAAAGGCT GAAAAAACCAGCAAAAACCCACAAAAAAGT
nTh_r	5'-Phos-GGGTTTTTGCTGGTTTTTTCAGCCTTTTTCGCCGTT TTTTGTGTCTTTTTGGGTCTTTTTTGC
210-bp rotor ring	
JV210_r	5' Phos-TCTTTTTTGGTCCTTTTTGCGACTTTTTTCGGCGTTT TTCTGCCTTTTTTGCGTGTTTTTGACCCTTTTTTCGCAGTTTTTGGC
JV210_1f	5'Phos-AAAGCTGCAAAAAAGAGCCAAAAACTGCGAAAAAA GGGTCAAAAACACGCAAAAAAGGCAGAAAAA
JV210_2f	5'Phos-CGCCGAAAAAAGTCGCAAAAAGGACCAAAAAAGAC TGAAAAATTCGCAAAAAACGGCGAAAAAGGC
ALgP_f	5'-Phos-AACCCACAAAAAAGTGACAAAAATGCGTAAAAAAT CTCCCTATAGTGAGTCGTATTAATTAA
JVgmblong	5'-Phos-ACTTTTTTGTGGGTTTTTGAGGCCGCGTTCAGCCTTTTTCGCCGTT TTTTGCGAATTTTTCAG
ALgP_r	5'-Phos- TCTTTTTTGCAGCTTTTTAATTAATACGACTCACTA TAGGGAGATTTTTTACGCATTTTTGTC
JVRO2short_f RO_rotor	5'-phosTGAACGCGGCCTCAAA
168-bp ring stator (with and without the Zif268 binding site)	
Alfa-b1zif	5'-phos-CGCCCACGCTGAACCCTTCGGAAAAAACGCGCAA AAAGCGCGAAAAAAGGG
Alfa-b1 nozif	5'-phos-AAAAAAGTGCCAAAAAGACGGAAAAAACGCGCAAA AAGCGCGAAAAAAGGGTTTTGA
168Beta rc	5'phos-AACATTTTTTGACAGTTTTTCCGTCTTTTTTGCGCGT TTTTCCATATTTTTTGAACATTTTTCTCCGTT
168Alpha2 r	5'phos-CAGTTTTTGGCCCTTTTTTCGCGCTTTTTGCGCGTTTT

	TTCCG
Alfa-a1zif2 Threading ODN	5’-phos-AAGGGTTCAGCGTGGGCGCCGCGGCCTCAACCGTTT TTTACCGCTTTTTG
Beta f short	5'phos-CCAAAAACTGTCAAAAAACGGAGAAAAATGTTCAAA AAATAT
Alfa b3long	5-phos-GGAAAAACGCGCAAAAAAGACGGAAAAACTGTCAA AAAATGTTCAAAAAGCGGTAAAAAAC
RO CAT2 RO_stator	5’-phos-GGTTGAGGCCGCGG
168-bp ring stator for the DNA catenane walker (substitute 168Beta rc by:)	
168beta rc_1short	5’-Phos- AACATTTTTTGACAGTTTTTCCGTCTTTTTTGGCTGACCTCCA
168beta rc2cshort	5’-Tamra- GCGATGAGGCCGCGTTCAGCCTGGAGGTCAGCTT TTTCCATATTTTTTGAACATTTTTCTCCGTTTTTTGA
Blocker rc2c	5'-ACGCGGCCTCATCGCATTACATCATGGT
RO_Blocker rc2c	5'-ACCATGATGTAATGCGATGAGGCCGCGT
ODNs for the catenane walker/Steps on DNA origami path and comp-iStep	
Step1_6HB_JV34	5'-ACACCGCCTGCAACAAGATGATGAAACAAAACACCGGA ATCATTATTATTATTGGCTGAACGCGGCCTCAAAAACCCACAAAA AA
Step2b_6HB_JV40	5'-ATTAAATCCTTTGCCAATATAATCCTGACCTGTTTATCA ACATTTTATTTATGCCTCATCGCCT-BHQ2-3‘
Step2b_6HB_JV51	5'-CAAACGGCGGATTGCATTCCATATAACATCAGTTGAGA TTTATTTTATTTATGCCTCATCGCCT-BHQ2-3‘
iSteplong1_6HB_JV91	5‘(Cy5)-AAAGACTGAAAAATTCGCAAAAAACGGCTTATATG TGATAAATAAGGATCCAAATAAGAAAAACGTAGAAAATAC
iSteplong2_6HB_JV92	5‘(Cy5)-AAAGACTGAAAAATTCGCAAAAAACGGCTTATATA ATTACTAGAAAAAATTTGCCAGTTACAACGCAAAGACACC
iSteplong2_6HB_JV92 (HEX)	5‘(HEX)-AAAGACTGAAAAATTCGCAAAAAACGGCTTATATA ATTACTAGAAAAAATTTGCCAGTTACAACGCAAAGACACC
iSteplong3_6HB_JV93	5‘(Cy5)-AAAGACTGAAAAATTCGCAAAAAACGGCTTATAAA ATTCTTACCAGTTCCTGAATCTTACCATAGAAAATTCATA
iSteplong4_6HB_JV95	5‘(Cy5)-AAAGACTGAAAAATTCGCAAAAAACGGCTTATAG GCAGAGGCATTTTGTTTTAGCGAACCTAAATTATTCATTAA
iSteplong5_6HB_JV98	5'(Cy5)-AAAGACTGAAAAATTCGCAAAAAACGGCTTATAA TAGATAAGTCCTGAACCAAGTACCGCAATAGCAGCACCGTA
iSteplong5_6HB_JV98 (FAM)	5'(FAM)-AAAGACTGAAAAATTCGCAAAAAACGGCTTATAAT AGATAAGTCCTGAACCAAGTACCGCAATAGCAGCACCGTA
iSteplong7_6HB_JV104	5'(Cy5)-AAAGACTGAAAAATTCGCAAAAAACGGCTTATAAG GCTTGCCCTGACAAGACTTTTTCATGACAGGAGGTTGAGG
iSteplong7_6HB_JV104(TxR)	5'(TexasRed)-AAAGACTGAAAAATTCGCAAAAAACGGCTTAT AAGGCTTGCCCTGACAAGACTTTTTCATGACAGGAGGTTGAGG
iSteplong8_6HB_JV107	5'-(Cy5)- AAAGACTGAAAAATTCGCAAAAAACGGCTTATACGTTGGGAAGA AAAAACCGATATATTCGGATGATACAGGAGT
Comp i-step new	5‘ AATTTTTCAGTCT (BHQ3) 3‘
Comp i-step	5' CGAATTTTTCAGTCTTATTA (biotin)-3'

newbioE	
JVgmblong_RO	5' ACTTTTTTGTGGGTTTTTGAGGCCGCGTTCAGCCTTTTT
Displace_comp-i-step	5' TTTCGCCGTTTTTTGCGAATTTTTCAGTCTTT
ODNs for the catenanes used in smFRET experiments	
JVgmblong (icy3)	5‘-Phos-ACTTTTTTGTGGGTTTTTGAGGCCGCGTTCAGCCT TT(icy3)TTCGCCGTTTTTTGCGAATTTTTCAG
Alfa-a1zif2(icy5)	5’-phos-AAGGGT(icy5)TCAGCGTGGGCGCCGCGGCCTCAACC GTTTTTTACCGCTTTTTG
168beta rc2cshort (biotin)	5’-Biotin-TTTGGAGGTCAGCTTTTTCCATATTTTTTGAACAT TTTTCTCCGTTTTTTGA
168beta rc_1short	5’-Phos-AACATTTTTTGACAGTTTTTCCGTCTTTTTTGGCTGA CCTCCA
Molecular beacon ODN (2’-OMe-RNA)	
MB	5’-FAM-UUUGCCUGAAAAAUUCGCAAA-Dabcyl-3’
ODNs used for SPR measurements	
Long N/Z_JV	5‘-Biotin-TTTTTTTTTTTTTTTTCTGCAAGGGTTCAGGCG TGGGCGGTAAG-3‘
N/Z_JV_rev	5‘-CTTACCGCCCACGCCTGAACCCTTGCAGA

Supplementary Table 2: Gamma function fitting parameters for the full transcription cycle and the FRET transition times

Rotor	Shape factor or number of irreversible steps	Dwell time in each step (s)	Dwell time after correction for the limited time window (s)
126-bp rotor (Full transcription cycle)	2.7 ± 1.2	192 ± 87	220
210-bp rotor (Full transcription cycle)	3.2 ± 0.6	155 ± 29	172
126-bp rotor (high FRET to low FRET)	2.0 ± 0.4	0.69 ± 0.19	0.69
126-bp rotor (low FRET to high FRET)	2.3 ± 0.6	0.45 ±0.14	0.45
210-bp rotor (high FRET to low FRET)	2.0 ± 0.4	0.51 ± 0.14	0.51
210-bp rotor (low FRET to high FRET)	2.6 ± 0.5	0.29 ± 0.06	0.29

Supplementary Table 3. ODNs for the catenane walker/DNA origami path

Name	Sequence
6HB_JV1	TACATTTTGACGCTATCTTACCGAAGCCCGCTAATATCAGAG
6HB_JV2	ACCGCCAGCCATTGAACAAAGTTACCAGGAATTAACTGAACA
6HB_JV3	ACTCAAACTATCGGGGAATACCCAAAAGCAGAGAGAATAACA
6HB_JV4	ACTTCTTTGATTAGGCAGTATGTTAGCACGATTTTTTGTTTA
6HB_JV5	TAAAAGAGTCTGTCCAACATATAAAAGAAAAATAAACAGCCA
6HB_JV6	AGAATCCTGAGAAGTTTTGTCACAATCAAACGCTAACGAGCG
6HB_JV7	CAGGAGGCCGATTACAAAGACAAAAGGGTGCTATTTTGCACC
6HB_JV8	GTATAACGTGCTTTGTAAATATTGACGGCCCGACTTGCGGGA
6HB_JV9	GCGCCGCTACAGGGCGTCACCGACTTGACTTATCCGGTATTC
6HB_JV10	GCGGTCACGCTGCGCACCAGTAGCACCAATCATTACCGCGCC
6HB_JV11	AAGAAAGCGAAAGGCAATGAAACCATCGCTCATCGAGAACAA
6HB_JV12	GCTTGACGGGGAAAAATCAAGTTTGCCTTTCCTTATCATTCC
6HB_JV13	AAAGCACTAAATCGCGGCATTTTCGGTCGTCGAAATCCGCGA
6HB_JV14	GAACCATCACCCAATTTCATAATCAAAAACAAAGTACAACGG
6HB_JV15	ACGTCAAAGGGCGACGCCTCCCTCAGAGAAACACTCATCTTT
6HB_JV16	CAGTTTGGAACAAGAGCCACCACCCTCAGAAGGCACCAACCT
6HB_JV17	ATAAATCAAAAGAACGCCGCCAGCATTGAGGAAGTTTCCATT
6HB_JV18	AAATCCTGTTTGATGGCCTTGATATTCAGCAACGGCTACAGA
6HB_JV19	AGTTGCAGCAAGCGAATGGAAAGCGCAGTCGTCACCCTCAGC
6HB_JV20	ACGGGCAACAGCTGCATACATGGCTTTTGTCGCTGAGGCTTG
6HB_JV21	TGCGTATTGGGCGCTTTTAACGGGGTCAACAATGACAACAAC
6HB_JV22	AGCTGCATTAATGACAGTTAATGCCCCCGAGGTGAATTTCTT
6HB_JV23	TGCGCTCACTGCCCACATGAAAGTATTACAAAAGGAGCCTTT
6HB_JV24	CCTGGGGTGCCTAATAGGATTAGCGGGGATAATAATTTTTTC
6HB_JV25	CAATTCCACACAACCGTCGAGAGGGTTGCAGCGGAGTGAGAA
6HB_JV26	CATGGTCATAGCTGCACCGTACTCAGGAAATTTTCTGTATGG
6HB_JV27	CGACTCTAGAGGATCACCCTCAGAACCGAACGATCTAAAGTT
6HB_JV28	GGTTTTCCCAGTCACGACGTTGTAAAACGACGGCAGGGATAG CAAGCCAACGCCTGTAGCA
6HB_JV29	AGTCACACGACCAATTTATCA
6HB_JV30	GAGATAGAACCCTTTAGCGATAGCTTAGGCTTAGGTTGGGTT
6HB_JV31	ACAGACAATATTTTTCGTCGCTATTAATATCCAATCGCAAGA
6HB_JV32	ACTGATAGCCCTAACATAAATCAATATAATATTTTAGTTAAT
6HB_JV33	CCACCAGCAGAAGATTAACAATTTCATTTGAAATACCGACCG
6HB_JV34	ACACCGCCTGCAACAAGATGATGAAACAAAACACCGGAATCA
6HB_JV35	GAAAAATCTAAAGCCGCGCAGAGGCGAACATATGCGTTATAC
6HB_JV36	CCCTCAATCAATATTAACGGATTCGCCTCAACAGTAGGGCTT
6HB_JV37	AGGAATTGAGGAAGATGAATATACAGTACAACATGTAATTTA
6HB_JV38	ACAACTAATAGATTCAGAAATAAAGAAAGAGAATATAAAGTA
6HB_JV39	GATTTAGAAGTATTAAGGGTTAGAACCTGACGACGACAATAA
6HB_JV40	ATTAAATCCTTTGCCAATATAATCCTGACCTGTTTATCAACA
6HB_JV41	GTAACATTATCATTAATTATCATCATATTATCCCATCCTAAT
6HB_JV42	TCAACCGTTCTAGCAAAGGCCGGAGACAGCCGGAACGAGGCG

6HB_JV43	ATTTTTGAGAGATCCAATGCCTGAGTAATGACCAACTTTGAA
6HB_JV44	AGTCTGGAGCAAACCGCAAGGATAAAAAGGCGCATAGGCTGG
6HB_JV45	ACTAGCATGTCAATTATGACCCTGTAATAGAACCGGATATTC
6HB_JV46	AGCCCCAAAAACAGAAGCCTCAGAGCATTCATTCAGTGAATA
6HB_JV47	GTAAACGTTAATATAATCATACAGGCAACGAGTAGTAAATTG
6HB_JV48	TAAATCAGCTCATTTGGCATCAATTCTAATCATTGTGAATTA
6HB_JV49	TAATTCGCGTCTGGCCTGTTTAGCTATATATACCAGTCAGGA
6HB_JV50	TAAATGTGAGCGAGATTTAGTTTGACCAAACGAACTAACGGA
6HB_JV51	CAAACGGCGGATTGCATTCCATATAACATCAGTTGAGATTTA
6HB_JV52	AGATGGGCGCATCGCATGTTTTAAATATCATAACGCCAAAAG
6HB_JV53	CGACGACAGTATCGATGGCTTAGAGCTTTATCATAACCCTCG
6HB_JV54	TTTCCGGCACCGCTGTACCTTTAATTGCAGCGAGAGGCTTTT
6HB_JV55	ATTCGCCATTCAGGGAACCAGACCGGAATAGTAAAATGTTTA
6HB_JV56	TGCGGGCCTCTTCGCGAAAGACTTCAAACGTCATAAATATTC
6HB_JV57	GTGCTGCAAGGCGACAGAAGCAAAGCGGGTTCAGAAAACGAG
6HB_JV58	AAGAGTCAATAGTGAGTAATAAAAGGGAGGATTATTTACATTGGCA GATTCACC
6HB_JV59	AATCCTTGAAAACACTGACCTGAAAGCGCTCATGGAAATACC
6HB_JV60	CTTGCTTCTGTAAATGAATGGCTATTAGTCCAGAACAATATT
6HB_JV61	TAATGGAAACAGTAAACATCGCCATTAAGCCTGAGTAGAAGA
6HB_JV62	AAAATTAATTACATTAAAACAGAGGTGAACCGTTGTAGCAAT
6HB_JV63	TACCTGAGCAAAAGAGTGCCACGCTGAGGTGAGGCCACCGAG
6HB_JV64	CCAAGTTACAAAATATCACCTTGCTGAAAGGAACGGTACGCC
6HB_JV65	ATCGGGAGAAACAACTGGTCAGTTGGCAGAGCGGGAGCTAAA
6HB_JV66	AGGTTTAACGTCAGGTTATCTAAAATATGCTTTGACGAGCAC
6HB_JV67	ATTTGCACGTAAAAAGAGCCGTCAATAGCCGCCGCGCTTAAT
6HB_JV68	CTTCTGAATAATGGAGACTTTACAAACACGCTGGCAAGTGTA
6HB_JV69	TGATGGCAATTCATCCGAACGTTATTAACGAGAAAGGAAGGG
6HB_JV70	ACCAGAAGGAGCGGTTGCGGAACAAAGAGCCCCCGATTTAGA
6HB_JV71	TTCAAAAGGGTGAGTGATAAATTAATGCGGTCGAGGTGCCGT
6HB_JV72	ATATATTTTAAATGTACAAAGGCTATCAATGGCCCACTACGT
6HB_JV73	AGCCTTTATTTCAAAAGAGAATCGATGAGAACGTGGACTCCA
6HB_JV74	TGTACCAAAAACATCATATGTACCCCGGGTTGAGTGTTGTTC
6HB_JV75	AAAATTAAGCAATAGAAGATTGTATAAGCGGCAAAATCCCTT
6HB_JV76	ATTAACATCCAATATTTGTTAAAATTCGGCCCCAGCAGGCGA
6HB_JV77	GCGAGCTGAAAAGGTTTTAACCAATAGGCCTGGCCCTGAGAG
6HB_JV78	CAAATGGTCAATAACCTTCCTGTAGCCATTTTCACCAGTGAG
6HB_JV79	CTGCGAACGAGTAGTAACAACCCGTCGGGGGGAGAGGCGGTT
6HB_JV80	GTGTCTGGAAGTTTACCGTAATGGGATAAAACCTGTCGTGCC
6HB_JV81	ATGCTGTAGCTCAATAACCGTGCATCTGCACATTAATTGCGT
6HB_JV82	GGTCATTTTTGCGGGCCTCAGGAAGATCCATAAAGTGTAAAG
6HB_JV83	GTCAGGATTAGAGATCTGGTGCCGGAAATTGTTATCCGCTCA
6HB_JV84	TCGAGCTTCAAAGCCTGCGCAACTGTTGCTCGAATTCGTAAT
6HB_JV85	ATTAAGAGGAAGCCCTATTACGCCAGCTGCATGCCTGCAGGT
6HB_JV86	GTCTTTACCCTGACTATTATAGTTTAAGTTGGGTAACGCCAG
6HB_JV87	AAATCATAGGTCTGAGAGACTACAATTGAGTTAAGCCCAATA

6HB_JV88	ATATAACTATATGTAGAGGGTAATTGAGCTTTTTAAGAAAAG
6HB_JV89	CAAAGAACGCGAGACGCATTAGACGGGAAAGGAAACCGAGGA
6HB_JV90	TTCATCTTCTGACCAATAGCAGCCTTTAAACTGGCATGATTA
6HB_JV91	TGTGATAAATAAGGATCCAAATAAGAAAAACGTAGAAAATAC
6HB_JV92	TAATTACTAGAAAAAATTTGCCAGTTACAACGCAAAGACACC
6HB_JV93	AAATTCTTACCAGTTCCTGAATCTTACCATAGAAAATTCATA
6HB_JV94	AATTGAGAATCGCCAAATCAAGATTAGTCGACATTCAACCGA
6HB_JV95	GGCAGAGGCATTTTGTTTTAGCGAACCTAAATTATTCATTAA
6HB_JV96	CCGACAAAAGGTAATCAGATATAGAAGGGCCATTTGGGAATT
6HB_JV97	ACAACATGTTCAGCTTTTCATCGTAGGATTACCATTAGCAAG
6HB_JV98	ATAGATAAGTCCTGAACCAAGTACCGCAATAGCAGCACCGTA
6HB_JV99	TTACGAGCATGTAGATAATCGGCTGTCTTTAGCGTCAGACTG
6HB_JV100	CAGACGGTCAATCAGCCTGATAAATTGTATAGCCCCCTTATT
6HB_JV101	AGAGGACAGATGAAATACCAAGCGCGAATCACCGGAACCAGA
6HB_JV102	CTGACCTTCATCAAAAAAGAATACACTACCGCCACCCTCAGA
6HB_JV103	ATTACCCAAATCAACGTAATGCCACTACGAGCCGCCACCAGA
6HB_JV104	AGGCTTGCCCTGACAAGACTTTTTCATGACAGGAGGTTGAGG
6HB_JV105	GGCTTGAGATGGTTTCGGAACGAGGGTACAAACAAATAAATC
6HB_JV106	CCTTATGCGATTTTCCGCTTTTGCGGGATCTCTGAATTTACC
6HB_JV107	CGTTGGGAAGAAAAAACCGATATATTCGGATGATACAGGAGT
6HB_JV108	ACAACATTATTACACGATAGTTGCGCCGGTGCCTTGAGTAAC
6HB_JV109	GGAATACCACATTCATCAGCTTGCTTTCTGCCTATTTCGGAA
6HB_JV110	GAATTACGAGGCATCAAAAAAAAGGCTCAGAGGCTGAGACTC
6HB_JV111	TTTACCAGACGACGTAAAGGAATTGCGATTTTGCTCAGTACC
6HB_JV112	GCAAAAGAAGTTTTACTTTCAACAGTTTATATAAGTATAGCC
6HB_JV113	GACTGGATAGCGTCGACGTTAGTAAATGGGTTTAGTACCGCC
6HB_JV114	ATTGAATCCCCCTCCTCATAGTTAGCGTCCACCCTCAGAGCC
6HB_JV115	AATGACCATAAATCACCAGTACAAACTACCAATAGGAACCCA TGTACCGTAACA
6HB_JV116	AGATAACCCACAAGCTTTTTAACCTCCGATTAAGACGCTGAG
6HB_JV117	CCCTGAACAAAGTCAAATGCTGATGCAATAATTTTCCCTTAG
6HB_JV118	TAAAAACAGGGAAGAAACTTTTTCAAATTGTGAGTGAATAAC
6HB_JV119	ACGTCAAAAATGAATAAATTTAATGGTTTGAATTACCTTTTT
6HB_JV120	TATTATTTATCCCACGTTAAATAAGAATAACATCAAGAAAAC
6HB_JV121	TCTTTCCAGAGCCTAGCCTGTTTAGTATTTATTCATTTCAAT
6HB_JV122	CAGCTACAATTTTAATAAAGCCAACGCTGATTGCTTTGAATA
6HB_JV123	GGTTTTGAAGCCTTATATTTAACAACGCACAGTACCTTTTAC
6HB_JV124	TAAGAACGCGAGGCCGAGCCAGTAATAATTGCGTAGATTTTC
6HB_JV125	CAATAGCAAGCAAAAGTAATTCTGTCCAACCATATCAAAATT
6HB_JV126	GCAAGCCGTTTTTATAATGCAGAACGCGTTGTTTGGATTATA
6HB_JV127	AAGAACGGGTATTAAACAAGAAAAATAATCCTGATTATCAGA
6HB_JV128	CCTGCTCCAAATCAAAACCTGTTACTTAGTCAAATCACCACC
6HB_JV129	AGATTTGTATCATCTAAGGGAACCGAACTGTGTAGGTAAAGA
6HB_JV130	GACCCCCAGCGATTCGGTGTACAGACCATTTTTAGAACCCTC
6HB_JV131	AAAACGAAAGAGGCGAGTAATCTTGACAACTTTTGCGGGAGA
6HB_JV132	AAACGGGTAAAATACGTAACAAAGCTGCAAAGCTAAATCGGT

6HB_JV133	GGCTTTGAGGACTAGAGAAACACCAGAAGGCAAAGAATTAGC
6HB_JV134	CAGGGAGTTAAAGGAAGAACTGGCTCATTTTTCATTTGGGGC
6HB_JV135	CATCGCCCACGCATATCTACGTTAATAATTAGATACATTTCG
6HB_JV136	AAACAGCTTGATACGGTAGAAAGATTCAGTTGATTCCCAATT
6HB_JV137	AATTGTATCGGTTTAACTAATGCAGATAGCAACTAAAGTACG
6HB_JV138	ACGTTGAAAATCTCAGTAAGAGCAACACAATTGCTGAATATA
6HB_JV139	TAGAAAGGAACAACATAAAAACCAAAATTCCTTTTGATAAGA
6HB_JV140	GATTTTGCTAAACAGCCAGAGGGGGTAAGCAAACTCCAACAG
6HB_JV141	TTGTCGTCTTTCCACAATACTGCGGAATTATCGCGTTTTAAT
6HB_JV142	TTCCACAGACAGCCAAATGCTTTAAACAATTGCATCAAAAAG
6HB_JV143	CTGAGTTTCGTCAAAAATCAG
6HB_JV144	AGCGAAAGACAGCATAATTTCAACTTTACTAATAGTAGTAGC
6HB_JV145	ATAAGAGCAAGAAACAATGAAATAGCAATAGCTCAATCG TCTGAAATCATTCTGGCCAACA
6HB_JV146	TAAGCAGATAGCCGCAACAGGAAAAACGTAAGAATACGTGGC
6HB_JV147	AACGCAATAATAACCCTTGCTGGTAATATCTTTAATGCGCGA
6HB_JV148	AGACTCCTTATTACTAATAACATCACTTAAATACCGAACGAA
6HB_JV149	ATACATAAAGGTGGCATCACGCAAATTAGGCGGTCAGTATTA
6HB_JV150	ACGGAATAAGTTTATGTTTTTATAATCAAGCCAGCAGCAAAT
6HB_JV151	TGGTTTACCAGCGCAAGGGATTTTAGACCCTCAAATATCAAA
6HB_JV152	TTGAGGGAGGGAAGCCTCGTTAGAATCAAATCAACAGTTGAA
6HB_JV153	AGGTGAATTATCACCGCGTACTATGGTTCTTTAGGAGCACTA
6HB_JV154	AGAGCCAGCAAAATCGTAACCACCACACATAATACATTTGAG
6HB_JV155	GCCGGAAACGTCACAGCGGGCGCTAGGGATTCGACAACTCGT
6HB_JV156	ATCAGTAGCGACAGGCCGGCGAACGTGGTTTTAAAAGTTTGA
6HB_JV157	TAGCGCGTTTTCATGAACCCTAAAGGGAAATCAATATGATAT
6HB_JV158	AGCGTTTGCCATCTATCAAGTTTTTTGGCGGAGAGGGTAGCT
6HB_JV159	GCCACCACCGGAACAAAACCGTCTATCAGGTCATTGCCTGAG
6HB_JV160	ACCGCCACCCTCAGAGTCCACTATTAAAACGGTAATCGTAAA
6HB_JV161	ACCACCACCAGAGCTAGCCCGAGATAGGTTGATAATCAGAAA
6HB_JV162	CAGGTCAGACGATTGGTGGTTCCGAAATCAAATATTTAAATT
6HB_JV163	CTCATTAAAGCCAGGTCCACGCTGGTTTCATTAAATTTTTGT
6HB_JV164	GTTCCAGTAAGCGTATTGCCCTTCACCGAACGCCATCAAAAA
6HB_JV165	GTACTGGTAATAAGCAGGGTGGTTTTTCGCTTTCATCAACAT
6HB_JV166	AGTGCCCGTATAAAATCGGCCAACGCGCATTCTCCGTGGGAA
6HB_JV167	CCTATTATTCTGAAGCTTTCCAGTCGGGGGTCACGTTGGTGT
6HB_JV168	CTCAAGAGAAGGATTGAGTGAGCTAACTCCAGTTTGAGGGGA
6HB_JV169	AGGCGGATAAGTGCATACGAGCCGGAAGGCACTCCAGCCAGC
6HB_JV170	CGGAATAGGTGTATTTTCCTGTGTGAAACCAGGCAAAGCGCC
6HB_JV171	ACCCTCAGAACCGCCCCCGGGTACCGAGGGAAGGGCGATCGG
6HB_JV172	ACCACCCTCATTTTCCAGTGCCAAGCTTGGCGAAAGGGGGAT

Supplementary Table 4. AFM analysis of Qdot attachment on the DNA origami path. Total number and percentage of DNA path structures with 0, 1, 2 and 3 Qdot attached at different time points (0, 20, 40 and 150 min) during the transcription of the catenane walkers with 210-bp and 126-bp rotors, as well as the non-transcription control.

		Nº of structures				% of structures			
	Time (min)	with 0 Qdots	with 1 Qdot	with 2 Qdots	with 3 Qdots	with 0 Qdots	with 1 Qdot	with 2 Qdots	with 3 Qdots
Transcription with Catenane walker (210-bp rotor)	0	4	17	30	8	6,8	28,8	50,8	13,6
	20	32	46	20	2	32,0	46,0	20,0	2,0
	40	36	28	7	0	50,7	39,4	9,9	0,0
	150	62	11	1	0	83,8	14,9	1,4	0,0
No transcription control	0	7	38	43	9	7,2	39,2	44,3	9,3
	20	9	29	49	9	9,4	30,2	51,0	9,4
	40	4	15	18	7	9,1	34,1	40,9	15,9
	150	6	45	79	13	4,2	31,5	55,2	9,1
Transcription with Catenane walker (126-bp rotor)	0	2	28	18	5	3,8	52,8	34,0	9,4
	20	19	33	10	1	30,2	52,4	15,9	1,6
	40	25	9	2	1	67,6	24,3	5,4	2,7
	150	56	15	1	0	77,8	20,8	1,4	0,0

Supplementary Table 5. Quantification of Qdot specific attachment on the different iSteps of the DNA origami path by AFM imaging analysis. Total number and percentage of Qdot attached on the different iStep positions at different time points (0, 20, 40 and 150 min) during the transcription of the catenane walkers with 210-bp and 126-bp rotors, respectively, as well as the non-transcription control.

		Nº of Qdots in position			% of Qdots in position		
	Time (min)	**#1**	**#2**	**#3**	**#1**	**#2**	**#3**
Transcription with Catenane walker (210-bp rotor)	0	35	26	40	59,3	44,1	67,8
	20	15	41	36	15,0	41,0	36,0
	40	4	21	11	5,6	29,6	15,5
	150	5	5	3	6,8	6,8	4,1
No transcription control	0	47	46	74	54,2	22,9	25,0
	20	50	48	56	52,1	50,0	58,3
	40	20	23	29	45,5	52,3	65,9
	150	56	95	91	39,2	66,4	63,6
Transcription with Catenane walker (126-bp rotor)	0	17	33	29	32,1	62,3	54,7
	20	9	30	17	14,3	47,6	27,0
	40	4	7	5	10,8	18,9	13,5
	150	6	8	3	8,3	11,1	4,2

References:

1 Zadeh, J. N. *et al.* NUPACK: Analysis and design of nucleic acid systems. *J Comput Chem* **32**, 170-173, doi:10.1002/jcc.21596 (2011).

2 Mathews, D. H., Sabina, J., Zuker, M. & Turner, D. H. Expanded sequence dependence of thermodynamic parameters improves prediction of RNA secondary structure. *J Mol Biol* **288**, 911-940, doi:10.1006/jmbi.1999.2700 (1999).

3 Douglas, S. M. *et al.* Rapid prototyping of 3D DNA-origami shapes with caDNAno. *Nucleic Acids Res.* **37**, 5001-5006, doi:10.1093/nar/gkp436 (2009).